PG
Petroleum Geoscience

Research article

Published Online First

https://doi.org/10.1144/petgeo2020-099

Evaluating the segmented post-rift stratigraphic architecture of the Guyanas continental margin

Max Casson[1*], Jason Jeremiah[2], Gérôme Calvès[3], Frédéric de Ville de Goyet[4], Kyle Reuber[5], Mike Bidgood[6], Daniela Reháková[7], Luc Bulot[1,8] and Jonathan Redfern[1]

[1] North Africa Research Group (NARG), Department of Earth and Environmental Sciences, The University of Manchester, Williamson Building, Oxford Road, Manchester M13 9PL, UK
[2] Golden Spike Geosolutions Ltd, 20 Ten Acres Crescent, Stevenage, Hertfordshire SG2 9US, UK
[3] Géosciences Environnement Toulouse (GET), Université Toulouse III – Paul Sabatier, 14 avenue Edouard Belin, 31400 Toulouse, France
[4] PetroStrat Ltd, Tan-y-Graig, Parc Caer Seion, Conwy LL32 8FA, UK
[5] ION GeoVentures, 2105 CityWest Boulevard, Houston, TX 77042, USA
[6] GSS (Geoscience) Ltd, 2 Meadows Drive, Oldmeldrum, Aberdeenshire AB51 0GA, UK
[7] Department of Geology and Paleontology, Faculty of Natural Sciences, Comenius University in Bratislava, Mlynská dolina, Ilkovičova 6, 842 15 Bratislava, Slovakia
[8] Aix-Marseille Université–CNRS–IRD–Collège de France–INRA, CEREGE, Site Saint-Charles, Case 67, 3 Place Victor Hugo, 13331 Marseille Cedex 3, France
Present addresses: MC, Equinor ASA, Equinor Research Centre, Svanholmen 8, Forus, Norway
MC, 0000-0003-4241-3447; GC, 0000-0003-3829-131X; KR, 0000-0003-4168-2135; MB, 0000-0002-4310-2467; DR, 0000-0002-3569-9179; LB, 0000-0002-2817-9327; JR, 0000-0002-0536-1492
*Correspondence: mcass@equinor.com

Abstract: Segmentation of the Guyanas continental margin of South America is inherited from the dual-phase Mesozoic rifting history controlling the first-order post-rift sedimentary architecture. The margin is divided into two segments by a transform marginal plateau (TMP), the Demerara Rise, into the Central and Equatorial Atlantic domains. This paper investigates the heterogeneities in the post-rift sedimentary systems at a mega-regional scale (>1000 km). Re-sampling seven key exploration wells and scientific boreholes provides new data (189 analysed samples) that have been used to build a high-resolution stratigraphic framework using multiple biostratigraphic techniques integrated with organic geochemistry to refine the timing of 10 key stratigraphic surfaces and three megasequences. The results have been used to calibrate the interpretation of a margin-scale two-dimensional seismic reflection dataset, and to build megasequence isochore maps, structural restorations and gross depositional environment maps at key time intervals of the margin evolution.

Our findings revise the dating of the basal succession drilled by the A2-1 well, indicating that the oldest post-rift sequence penetrated along the margin is late Tithonian age (previously Callovian). Early Central Atlantic carbonate platform sediments passively infilled subcircular-shaped basement topography controlled by the underlying basement structure of thinned continental crust. Barremian–Aptian rifting in the Equatorial Atlantic, caused folding and thrusting of the Demerara Rise, resulting in major uplift, gravitational margin collapse, transpressional structures and peneplanation of up to 1 km of sediment capped by the regional angular Base Albian Unconformity. Equatorial Atlantic rifting led to margin segmentation and the formation of the TMP, where two major unconformities developed during the intra Late Albian and base Cenomanian. These two unconformities are time synchronous with oceanic crust accretion offshore French Guiana and in the Demerara–Guinea transform, respectively. A marine connection between the Central and Equatorial Atlantic is demonstrated by middle Late Albian times, coinciding with deposition of the organic-rich source rock of the Canje Formation (average total organic carbon 4.21%). The succession is variably truncated by the Middle Campanian Unconformity. Refining the stratigraphic framework within the context of the structural evolution and segmentation of the Guyanas margin impacts the understanding of key petroleum system elements.

Supplementary material: Photographs of sandstone petrography thin sections (Fig. S1); calcareous nannofossil plates (Fig. S2); palynology reports for A2-1 and FG2-1 (Fig. S3); taxonomy description of new species; sample table and organic geochemistry results (Table S1); and nannofossil distribution charts (Table S2) are available at https://doi.org/10.6084/m9.figshare.c.5280490

Received 14 September 2020; **revised** 8 January 2021; **accepted** 23 January 2021

Continental margins are heterogeneous at various scales, resulting in along-strike asymmetry and segmentation. First-order structural and tectonic segmentation is mainly related to pre-existing basement heterogeneity, often separated by long-lived weaknesses in the continental crust; subsequently modified by the rifting process (i.e. the magnitude and orientation of extension (β-factor): McKenzie 1978) and break-up magmatism (volcanic v. non-volcanic margins: Franke 2013). Post-rift passive-margin subsidence and sedimentation finally influences the overall margin architecture, but it is still largely controlled by the pre-existing structure and thermal subsidence (Clemson *et al.* 1997). Old segmented continental margins, and particularly marginal plateaus, record multiple rift-to-drift cycles and/or failed rifts related to the gradual fragmentation of supercontinents (Wilson cycle: Wilson 1966; Burk and Dewey 1974). Exemplified in the studied Guyanas continental margin of South America, caused by the opening of the Central Atlantic and succeeding transform-dominated Equatorial Atlantic, with oblique opening directions (Fig. 1a) (Reuber *et al.*

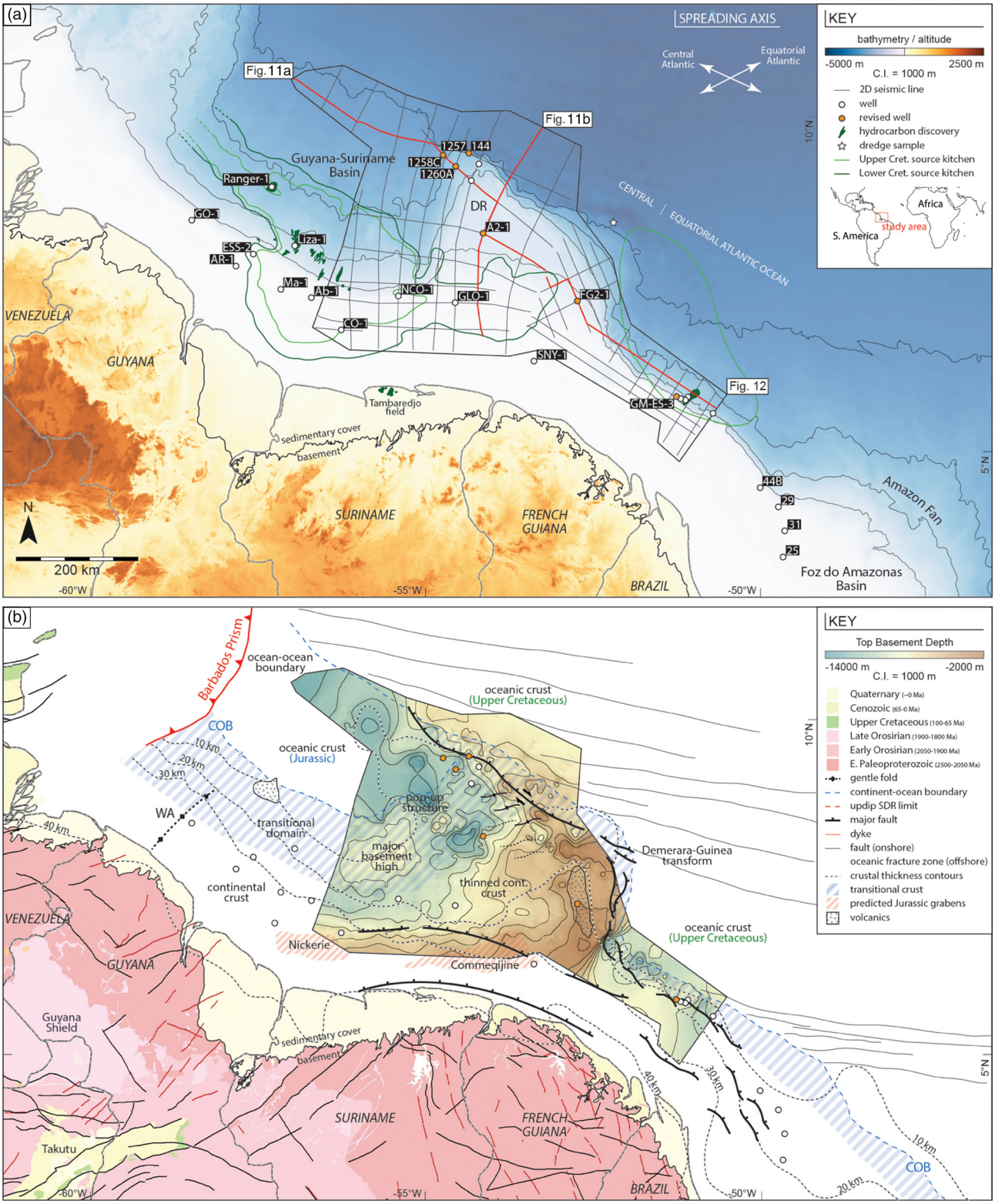

Fig. 1. (**a**) Shaded bathymetric and topographical location map of NE South America showing the structure of the Guyanas continental margin and subsurface dataset. Exploration wells and scientific boreholes used in this study are shown; orange circles highlight where new stratigraphic analysis has been performed. The ION Geophysical GuyanaSPAN 2D seismic reflection survey, the location of the composite seismic section (Fig. 11a), dip section SR1-5400 (Fig. 11b) and the isochore maps are shown (Fig. 12). Dredge samples recovered basalts and rhyolites zircon dated at 173.4 ± 1.6 Ma (Basile *et al.* 2020) from the seabed (white star). Onshore, the limit of sedimentary cover and, hence, the location of the Archean Guiana Shield is mapped (Cordani *et al.* 2016). Hydrocarbon discoveries and the limits of Cretaceous source kitchens after Kosmos Energy (2018). DR, Demerara Rise; WA, Waini Arch. (**b**) Structural framework of the Guyanas continental margin with a top basement depth–structure map interpreted from the ION Geophysical GuyanaSPAN 2D seismic reflection survey. The 'top basement' map was constructed from a merge between the top oceanic crust and top basement surfaces. The onshore geological map is from the geological map of South America (CGMW–CPRM–DNPM 2003). Structural features are mapped after Gouyet *et al.* (1994), Yang and Escalona (2011), Reuber *et al.* (2016) and Sapin *et al.* (2016); crustal thickness was modelled from 3D gravity anomaly inversion by Kusznir *et al.* (2018); predicted Jurassic graben offshore from Griffith (2017); and volcanics are from Gouyet *et al.* (1994) and Mourlot (2018).

2016). Conventional models of lithospheric thinning assume continuous post-rift subsidence (McKenzie 1978), yet more studies are revealing the dynamic nature of continental margins, with major post-rift vertical movements further influencing stratigraphic architecture (Morocco: Charton 2018; Mauritania: Gouiza *et al.* 2019; French Guiana: Derycke *et al.* 2018). All of these formative processes can invariably lead to a complex structural segmentation of the 'basement' (i.e. crust plus syn- and pre-rift strata) that subsequently controls post-rift depositional systems. Limited studies intrinsically address the margin-scale megasequence architecture in the complex geological setting of transform marginal plateaus (TMPs: *sensu* Loncke *et al.* 2020).

The Demerara Rise is a submarine promontory that extends for more than 200 km from the continental margin into the Atlantic Ocean (Fig. 1a) and has an African conjugate, the Guinea Plateau (Jacobi and Hayes 1982). Both features can be classified as TMPs covering a combined surface area of 92 000 km^2 due to the presence of a transform margin (Guinea–Demerara Fracture Zone) along one flank and the polyphased rifting history. The underlying basement characteristics have been analysed by documenting and interpreting a compilation of basement structures, which are displayed on the top basement structure map (Fig. 1b). This provides a model for the underlying structural framework to assess how basement inheritance may have controlled the structural evolution, subsidence and deposition of the studied overlying post-rift section (Fig. 1b).

Surrounding the Demerara Rise are thinned continental crust (Kusznir *et al.* 2018) and volcanic basement composed of seaward-dipping reflectors (SDRs: Reuber *et al.* 2016), the oceanic crust displays a diachronous accretion due to the dual-phase rifting history. Within the Guyana–Suriname Basin the oceanic crust is inferred to be Jurassic in age, whereas to the north and east of the Demerara Rise, in the Equatorial Atlantic domain, oceanic crust is at least 45 myr younger, accreted during the Upper Cretaceous (Fig. 1) (Basile *et al.* 2005; Reuber *et al.* 2016). Thus, the dual-phase rifting creates an apparent ocean–ocean boundary NW of the Demerara Rise where Jurassic and Upper Cretaceous oceanic crust is juxtaposed across the Demerara–Guinea transform. This heterogeneity is reflected in the basement morphology of the Demerara Rise, which is more complex than a typical continental margin (i.e. US Atlantic margin: Bally 1981), rising from subsurface depths below −12 000 m (old Jurassic oceanic crust) to −4000 m depth along the eastern margin of the Demerara Rise (Fig. 1b).

Investigating how the basement heterogeneity and structural inheritance subsequently controls post-rift sedimentation provides insights to better characterize the highly prospective world-class petroleum systems in the post-rift section, reducing uncertainty and risk for future exploration programmes. Our study integrates geological and geophysical approaches by refining the Mesozoic stratigraphic framework through resampling and analysis of exploration well data, and cores from the Deep Sea Drilling Project (DSDP) and Ocean Drilling Project (ODP) boreholes. This provides a template to constrain the timing of key stratigraphic events during the post-rift history. Results are then extrapolated to a margin-scale seismic reflection dataset to understand lateral (along-strike) heterogeneity and segmentation in depositional systems, which we predict were influenced by the dual-phase rifting and underlying structural inheritance.

Regional setting

The Guyanas continental margin of South America extends for 1500 km from the Barbados Prism in the west through the Guyana–Suriname Basin and across the Demerara Rise into the Equatorial Atlantic offshore French Guiana and the Foz do Amazonas Basin, Brazil (Fig. 1a). This margin is situated on the northeastern rim of the Archean Guiana Shield (Fig. 1b). The Demerara Rise, a prominent bathymetric feature, divides the margin into two tectonic domains, the Central Atlantic passive margin to the west and the Equatorial Atlantic transform margin to the east, marking the opening of North America and Africa, and South America and Africa, respectively. Consequently, the offshore stratigraphy records the opening of the Central Atlantic (170 Ma: Labails *et al.* 2010) and Equatorial Atlantic (105 Ma: Sibuet and Mascle 1978) as the African Plate rotated anticlockwise and rifted away from South America. Prior to this later rifting and the establishment of the Guinea–Demerara transform, the Demerara Rise formed the southern extension of the Guinea Plateau conjugate margin and, hence, the key study area for Atlantic Plate reconstructions (Pindell 1985; Moulin *et al.* 2010; Kneller and Johnson 2011; Heine *et al.* 2013). Jurassic post-rift sedimentation on the sutured southeastern margin of the Central Atlantic initiated with the establishment of an extensive, basin-fringing carbonate platform (Fig. 2) (Davison 2005). The southeastern extension of the Jurassic–Lower Cretaceous Central Atlantic Ocean formed an arcuate siliciclastic shoreline at the neck of the Equatorial Atlantic across the Demerara Rise (Gouyet *et al.* 1994).

Opening of the Equatorial Atlantic punctuated this tectonically-quiescent period of Jurassic–Lower Cretaceous passive-margin subsidence, which is expressed on the adjacent transform margin and on the West African conjugate as an Aptian unconformity associated with the onset of South Atlantic rifting (Sapin *et al.* 2016; Olyphant *et al.* 2017). Barremian–Aptian volcanism linked to Equatorial Atlantic break-up is locally developed on both the Guyanas (Gouyet 1988; Greenroyd *et al.* 2008) and African margins (Olyphant *et al.* 2017). The Equatorial Atlantic basins developed as a series of en echelon pull-apart basins separated by palaeodextral transform faults, now preserved as fracture zones (Pindell 1985; Greenroyd *et al.* 2007, 2008; Basile *et al.* 2013). Adjacent to this, on the northern margin of the Demerara Rise, compressional structural features are observed below a peneplaned Albian-aged angular unconformity (Gouyet 1988; Reuber *et al.* 2016). Transgression and opening of the Equatorial Atlantic gateway between the Central and South Atlantic followed (Gasperini *et al.* 2001; Friedrich and Erbacher 2006). Cenomanian–Coniacian organic-rich sediments were deposited along the Guyanas margin (Canje Formation) and in adjacent basins (i.e. Naparima Hill Formation, Trinidad; La Luna Formation, Venezuela and Colombia). These form prolific hydrocarbon source rocks (Erlich *et al.* 2003; Meyers *et al.* 2006). Thermal subsidence of the continental margin and denudation of the Guiana Shield resulted in increased sedimentation rates through the Late Cretaceous (Benkhelil *et al.* 1995; Yang and Escalona 2011; Mourlot 2018). Major uplift of the South American cratons led to the formation of the Purus Arch induced by Andean tectonism during the Paleogene–Miocene (Sapin *et al.* 2016). This initiated the transcontinental Amazon River, debouching significant volumes of sediment in a depocentre along the margin that persists to the present day (Fig. 1a) (Figueiredo *et al.* 2009).

Previous studies

The exploration well A2-1 drilled by Esso in 1978 reached total depth (TD) in reported Middle Jurassic-aged (Callovian: 166–163 Ma) sediments (Fig. 1a) (Staatsolie 2013), and, hence, was regarded as the oldest stratigraphic test. Significantly, as part of this study, we have redated the basal section of this well, determining a late Tithonian age (153–145 Ma) that is younger by at least 10 myr. Biostratigraphic detail and implications of the new age dating are provided later in this paper. This key well has been fundamental to the understanding of the stratigraphic evolution of the Guyana margin as the well records the oldest and most-complete post-rift stratigraphy (i.e. Gouyet 1988; Gouyet *et al.* 1994; Erbacher *et al.*

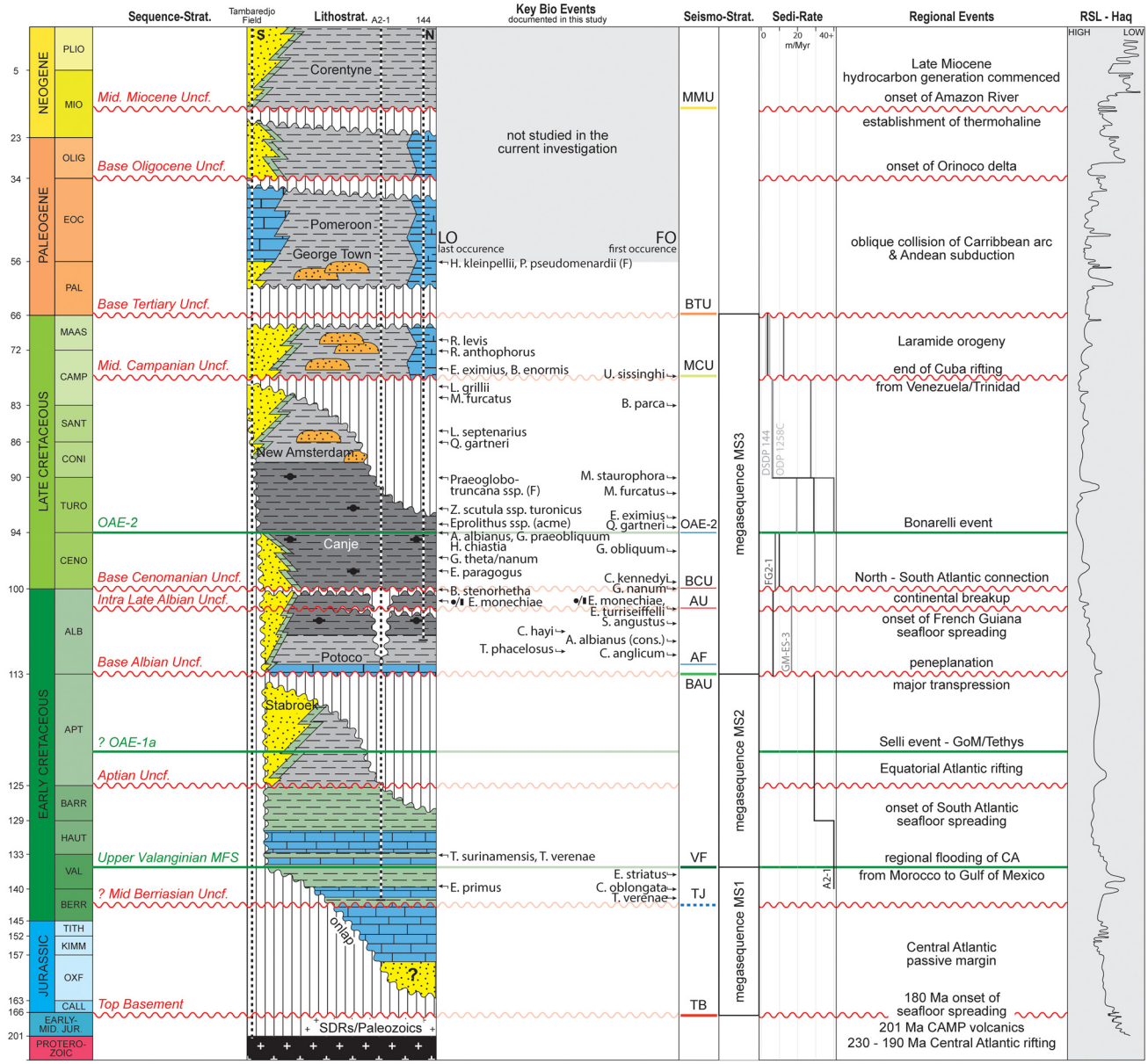

Fig. 2. Tectonostratigraphic framework for the Guyanas continental margin, offshore Suriname and Guyana. The major sequence-stratigraphic surfaces identified in this study are indicated, linked to key biostratigraphy events. Lithostratigraphy is based on seismic profile SR1-5400 (Fig. 11b) and is adapted from Nemčok *et al.* (2015); see the key in Figure 15. The main seismic markers and megasequences used in this study are highlighted. Calculated sedimentation rates (sedi-rates) are displayed in metres per million years (m Ma^{-1}). The relative sea-level curve is after Haq (2014). AF, Albian flooding surface; CAMP, Central Atlantic Magmatic Province; CF, Cenomanian flooding surface; OAE, oceanic anoxic event; SDRs, seaward-dipping reflectors; TB, top basement.

2004*a*; Kean 2007; Reuber *et al.* 2016; Griffith 2017). The DSDP collected data from the Cretaceous sequence to investigate the early evolution of the Central Atlantic on Leg 14 at Site 144 (Fig. 1a) (Hayes *et al.* 1972). More recently, the ODP studied the opening of the Equatorial Atlantic Gateway by drilling sites on Leg 207 (Fig. 1a) (Erbacher *et al.* 2004*a*). This provided the scientific community with core data from the Late Cretaceous–recent sequence, and subsequent studies have significantly improved the existing stratigraphic framework (Erbacher *et al.* 2004*a*, *b*,2005; Mosher *et al.* 2005; Friedrich and Erbacher 2006; Hardas and Mutterlose 2006; Kulhanek and Wise 2006; Thibault and Gardin 2006; Krauspenhar *et al.* 2014). Yang and Escalona (2011) used existing industry data to propose the tectonostratigraphic evolution of the Guyana–Suriname Basin. Post-Albian sedimentary evolution of the Demerara Rise is investigated in Tallobre *et al.* (2016) and Fanget *et al.* (2020), focusing on documentation of contourite deposits related to the North Atlantic Deep-Water current. Re-evaluating and integrating these data with our new results along the full extent of the margin strengthens our understanding of the stratigraphic evolution.

Dataset and methods

Data

Lithological samples

Resampling the DSDP Site 144 and ODP Leg 207 cores took place during 2017–18, at the IODP Bremen Core Repository, Germany (request ID: 054376IODP, 065859IODP and 077865IODP). Drill cutting samples from the exploration wells (A2-1, FG2-1 and GM-ES-3) were collected from the CGG Schulenburg facility, Houston, USA in 2018, kindly donated by Shell. The remainder of these samples are stored for reference in the North Africa Research Group collection at the University of Manchester. A sample summary is provided in Table S1 of the Supplementary material.

Subsurface seismic and well data

The seismic reflection data used in this study offshore NE South America consists of 34 2D seismic reflection profiles (a total of 7970 line km) from the ION Geophysical GuyanaSPAN survey (Fig. 1a). The survey imaged the entire continental margin in water depths of 40–3500 m, with a 50 m shot spacing, recording to 40 km depth and was provided as pre-stack depth migrated (PSDM) SEGY data. The Suriname–French Guiana ION data are reprocessed data using WiBand broadband technology, recording to 25 km depth. A comparison was made to the conjugate Guinea Plateau. Wireline logs (gamma ray (GR) and sonic) for the exploration wells were provided by Shell, and downloaded from the IODP data repository for ODP Leg 207.

Methods

A multidisciplinary approach has been adopted to investigate and integrate a large subsurface dataset with existing studies to document continental margin evolution.

Sedimentology and organic geochemistry

Drill cutting samples were set in resin and thin sectioned for petrographical analysis using an optical light microscope. Descriptive petrographical sandstone classification was performed after Garzanti (2016). Whole-rock X-Ray diffraction (XRD) was performed at BGS Keyworth on samples from FG2-1 using a PANalytical X'Pert Pro series diffractometer and the quantification methods of Snyder and Bish (1989).

Sixty-five shale samples were selected for organic geochemical analysis using a Shimadzu TOC-V CPN and Solid Sample Module (SSM), calibrated to sodium carbonate and glucose to measure inorganic and total carbon, respectively. Additional geochemical data for ODP Site 1258C was incorporated from Meyers *et al.* (2006). The TOC data generated from the analysis of cuttings (exploration wells) was expected to yield lower results due to the contaminant and mixing with other lithologies, compared to core data (DSDP Site 144).

Further geochemical characterization of 34 samples yielding >0.5% TOC was completed using a Rock-Eval 6 instrument at the University of Greenwich. Measurements of TOC were consistently less than TOC derived from the Rock-Eval by, on average, 0.53%. We report the results from the separate TOC analysis as this is often a more reliable measurement of TOC compared to results from the Rock-Eval 6 (see Behar *et al.* 2001). In addition, a solvent was not used to remove free hydrocarbons prior to the pyrolysis, whereas in the TOC analysis any free hydrocarbons are generally removed during the process, which leads to a higher value from the Rock-Eval.

Four samples from well A2-1 at Aptian and older levels with reported hydrocarbon shows were sent to GeoMark Research, Houston for hydrocarbon extract analysis. Extracts were analysed for high-resolution gas chromatography and biomarker geochemical analysis.

Biostratigraphy

Dependent on lithology, various biostratigraphic analyses were performed to provide age constraints on the stratigraphy. All key biostratigraphic events are shown in Figure 2, and Table S1 of the Supplementary material highlights which samples were analysed using the different techniques.

Calcareous nannofossils

In total, 138 samples (see Table S2 of the Supplementary material for the nannofossil event charts by well) were analysed with standard techniques described by Bown (1998), and the picking brush method of Jeremiah (1996). Samples were analysed semi-quantitatively, with the first 30 fields of view counted and the remaining slide scanned for rare specimens. Photographs of newly described and selected marker species are shown in Figure S2 of the Supplementary material and further text describing the taxonomy of new species is provided in the taxonomy document of the Supplementary material.

Foraminifera

Thirty-one samples with relatively abundant calcareous nannofossil content were chosen for micropalaeontological analysis and prepared using the standard methodology described by Armstrong and Brasier (2013).

Palynology

Ten samples for palynological analyses were subject to the standard palynological preparation technique, which involves removal of all mineral material by hydrofluoric acid digestion and sieving to produce a residue of the 10 µm and above size fraction for each sample. An initial count of 100 *in situ* palynomorph specimens was performed and abundance quantitatively assessed using the percentage of total palynoflora. The palynology charts are provided in Figure S3 of the Supplementary material.

Calpionellids

A total of eight limestone-rich cutting samples from well A2-1 were thin sectioned and petrographically analysed for the occurrence of calpionellids. Results are amalgamated within the 'dating' section of each well/borehole; therefore the letters (N), (F), (P) and (C) are used to denote the type of fauna, calcareous nannofossils, foraminifera, palynology, calpionellids, respectively, when discussed.

Cuttings samples are (theoretically) composited, representative material from a drilled interval of rock. Cuttings are susceptible to contamination from material collapsing into the borehole (called 'cavings') from levels higher in the section and contaminating *in situ* sample material from near the drill bit. To mitigate contamination from cavings, multiple picked lithologies per sample were analysed for nannofossils, the oldest sample being considered representative of the depth; first occurrence (FOs) and last occurrence datums (LOs) were then utilized. This was not possible for the palynology and foraminiferal work where more rock material is required; extinction events (or events which become apparent in a downhole perspective) form the basis for the majority of biostratigraphic determinations (i.e. first downhole occurrence (FDO)).

Seismic interpretation and structural evolution

To ensure a robust seismic-well tie and depth calibration, synthetic seismograms for two exploration wells, A2-1 and FG2-1, plus the ODP Leg 207 boreholes were produced. This process tied the wireline log data to the seismic survey following the methodology of Sheriff (1976, 1977). Despiked sonic logs were converted to give an estimation of the density log using Gardner's equation. Statistical wavelets were extracted for wells A2-1 and FG2-1 from the zones of interest: 2000–4000 and 2000–3500 m depth, respectively. Following this, key horizons (Fig. 2) identified during the stratigraphic re-evaluation were interpreted on the 2D seismic dataset using Schlumberger's Petrel software and the interpretation methods of Payton (1977). Horizons were gridded and isochore-thickness maps calculated for three gross megasequences. Flattening of the seismic section on key horizons helped to improve our understanding of depositional geometries and structural features at the time of deposition (Bland *et al.* 2004).

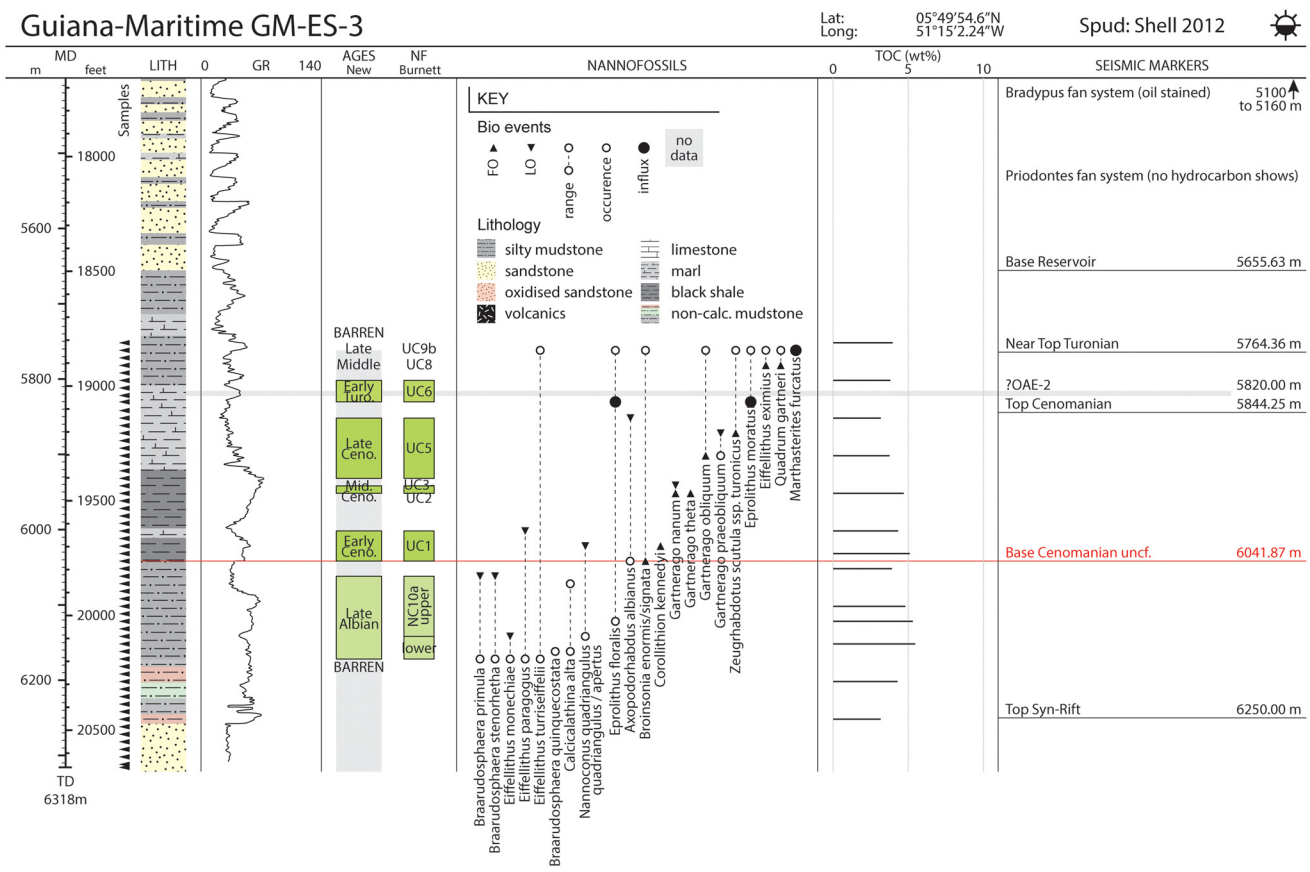

Fig. 3. A re-evaluation of the Guiana-Maritime GM-ES-3 well stratigraphy displaying nannofossil events (Table S2 of the Supplementary material), total organic carbon (TOC: Table S1 of the Supplementary material) measurements and key stratigraphic surfaces. The location is displayed in Figure 1a.

Projecting the uppermost continuous seismic reflector below the Base Albian Unconformity (BAU) provided an estimation for the amount of missing section due to erosion.

Results

Sedimentological and stratigraphic control

Seven wells and scientific boreholes in the study area provide the control on lithologies/facies, age dating and organic geochemistry. These have been re-examined and the new data used to build depositional models to constrain and be integrated into the seismic dataset. Sample depths are reported in the original unit of measurement, and a metric conversion is provided for imperial depth measurements.

GM-ES-3

Exploratory drilling offshore French Guiana targeted the Santonian–Maastrichtian-aged Cingulata turbidite fan system (McCoss 2017). Through 2011–13, 5 exploration wells were drilled with the first, GM-ES-1 (Zaedyus), encountering 72 m of net oil pay. Subsequent wells failed to find commercial hydrocarbons in adjacent prospects due to failure of the stratigraphic traps. This includes GM-ES-3 (Priodontes), which penetrated a 50 m gross section of oil-stained sandstone reservoir (Bradypus fan) above the targeted water-wet reservoir (Priodontes fan), well failure was as a result of an invalid trap. The 670 m-thick sequence below the reservoir section to TD is mudstone dominated with calcareous and organic-rich intervals. At 6036 m there is a lithology change from shale to non-calcareous mudstones and, at TD, sandstones, considered to be pre-rift strata. The data from this well provide crucial stratigraphic information of deposits recording the rift-to-drift transition and timing of break-up in the Equatorial Atlantic (Fig. 3).

Dating

The current study investigates the pre-Coniacian–Santonian reservoir section in GM-ES-3 (Fig. 3), all the age dating is based on calcareous nannofossils (N). The interval 5760–5830 m confirms a complete Turonian sequence. Penetration of the latest Turonian is confirmed at 5760 m with the presence of an influx of *Marthasterites furcatus* below the FO of *Micula staurophora*. An age no older than Middle Turonian is confirmed with the FO of *Eiffellithus eximius* at 5780 m. Earliest Turonian sediments characterized by the quantitative influx of *Eprolithus moratus* and *E. floralis* occur between 5800 and 5830 m, events below the FO of *Quadrum gartneri* at 5780 m. The Ocean Anoxic Event 2 (OAE-2) interval is postulated at *c.* 5820 m where there is a subtle peak in the GR log, probably subdued in comparison to other studied wells due to the turbidite input nearby (encountered in GM-ES-1). This occurs within Early-Turonian-aged sediments, typically latest Cenomanian with the top at the Cenomanian–Turonian boundary, we postulate this is either due to log to driller's discrepancy or just the rarity of top Cenomanian markers at this point. Penetration of Cenomanian-aged strata is proven by the LO of *Axopodorhabdus albianus* at 5850 m. Middle–Lower Cenomanian strata occur at 5940 m with the LOs of *Gartnerago nanum* and *G. theta*. The LO of consistent *Eiffellithus paragogus* at 6000 m confirms penetration of the Lower Cenomanian (Burnett 1998; Ando *et al.* 2015; Chin 2016), Cenomanian sediments are proven as deep as 6020–6040 m with the occurrence of *Corollithion kennedyi* and FOs of common *Broinsonia signata*.

The Upper Albian is confirmed at 6060 m, with the consistent LO of *Braarudosphaera* spp., including *B. stenorhetha*. The excellent preservation is reflected in the preservation of *B.*

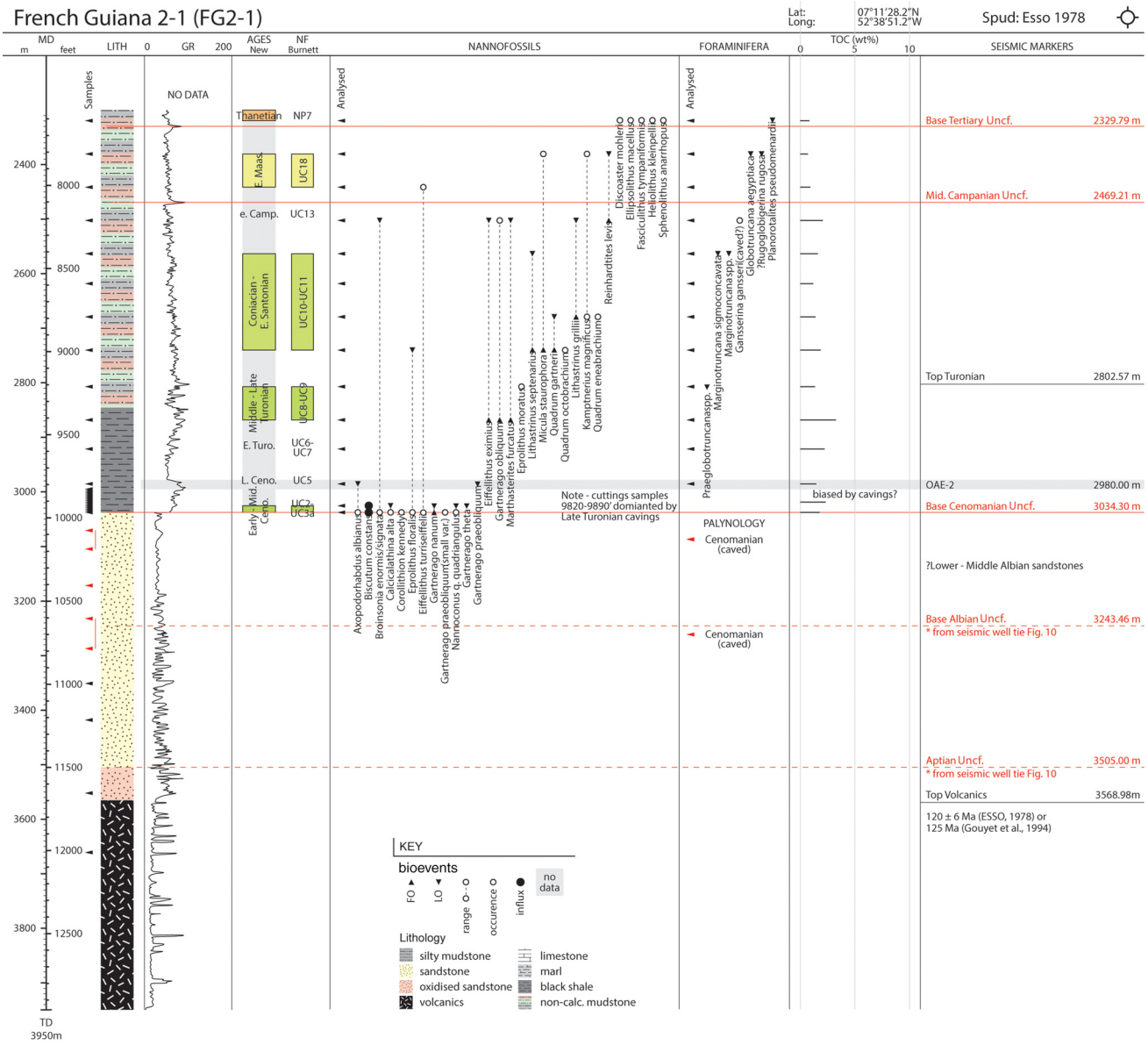

Fig. 4. A re-evaluation of the French Guiana 2-1 (FG2-1) well stratigraphy displaying nannofossil events (Table S2 of the Supplementary material), foraminifera and palynology results, total organic carbon (TOC: Table S1 of the Supplementary material) measurements, and key stratigraphic surfaces. The location is displayed in Figure 1a.

primula dodecahedra. A marked downhole increase in braarudosphaeres was recorded towards the top Albian from ODP Leg 171B, Site 1052E off the Blake Nose Plateau by Watkins *et al.* (2005); a similar top to a *Braarudosphaera quinquecostata* acme event from Texas and Oklahoma by Hill (1976), and downhole increase in *B. primula* often associated with *B. stenorhetha* from the offshore Gulf of Mexico (J. Jeremiah, pers. obs.) and offshore Morocco (Chin, 2016). Although *Nannoconus* spp., including *N. quadriangulus quadriangulus* and *N. q. apertus*, are consistently observed, the Late Albian quantitative acme recorded by Hill (1976) and Watkins *et al.* (2005) is not recorded from offshore Suriname.

GM-ES-3 is unusual in the current study in having a relatively expanded latest Albian section (NC10a upper) between 6060 and 6130 m. At 6140 m, the LO of *Eiffellithus monechiae* is recorded, its co-occurrence with equal numbers of *Eiffellithus turriseiffelii* down to 6170 m proving an age no older than the lower part of NC10 (Jeremiah 1996; Bown 2001; Gale *et al.* 2011). Marine Late Albian mudstones rest directly on non-marine rift sandstones at TD (palynology results from Shell).

French Guiana 2-1 (FG2-1)

Well FG2-1 was spud in 1978 by Esso, the main objective being Lower Cretaceous clastics and underlying carbonates in a structural closure. The well was dry, probably drilled off-structure in a hydrocarbon fairway shadow, and Late Cretaceous source rocks penetrated at the well were immature. Well FG2-1 is unique along the continental margin as it reaches TD in a 380 m-thick succession of basalts previously reported as 125 Ma (Barremian: Gouyet *et al.* 1994) (Fig. 1b) and 120 ± 6 Ma in age (Esso 1978). Whole-rock XRD shows the volcanics to have a mafic composition, predominantly plagioclase and pyroxene with smectite, chlorite, quartz and magnetite. Smectite is likely to have originated from weathered basalts. Approximately 50 m of oxidized red sands overlie this unit, suggesting subaerial exposure (Fig. 4). About 470 m of very-fine- to fine-grained litho-quartzose sandstone with clay matrix is encountered above this. Petrographical investigation reveals that the sands are poorly sorted and matrix supported, with sub-angular quartz grains and additional lithic clasts of reworked sedimentary material (see Fig. S1 of the Supplementary material). These sands were

likely to have been deposited in a non-marine/continental environment as no marine fauna or glauconite were observed in the petrographical analysis. At 3030 m depth, there is a lithological break recorded as a positive shift in the GR log; sediments above this surface are calcareous organic-rich mudstones recording the first marine-influenced strata.

Dating

Nannofossil and foraminifera analysis started at 7600 ft (2316.50 m) within lower Thanetian sediments, based on the co-occurrence of *Heliolithus kleinpellii*, *Discoaster mohleri* (N) and the FDO of *Globanomalina pseudomenardii* (F). This level is just above the Base Tertiary Unconformity (BTU) identified at 2329.79 m. Lower Paleocene and Upper Maastrichtian deposits appear to be missing; this sequence is not encountered in subsequent cavings. A diverse Lower Maastrichtian assemblage is recovered from the interval 7800–8000 ft (2377.4–2438.4 m) with *Reinhardtites levis* (N) recorded, supported by the FDO of *Globotruncana aegyptiaca* (F). At 8200 ft (2499.4 m) the LOs of *Marthasterites furcatus*, common *Eiffellithus eximius*, *Lithastrinus grillii* and *Broinsonia signata* (N) indicate basal Campanian deposits.

A relatively complete Santonian–Coniacian sequence is penetrated between 8400 and 8980 ft (2560.3–2737.1 m). At 8400 ft (2560.3 m) Lower Santonian deposits are proven with the LO of *Lithastrinus septenarius* (N). The LO of *Quadrum gartneri* and *Q. eneabrachium* (N) is at 8780 ft (2676.1 m), followed by the FO of *Micula staurophora* and LO of *Eprolithus floralis* (N) at 8980 ft (2737.1 m). This is supported by the foraminifera analysis where the FDO of *Marginotrucana sigmoconcavata* (F) indicates an age no younger than Santonian (intra-*Dicarinella asymetrica* zone) at 8400 ft (2560.3 m). The presence of common *Marginotruncana* spp. (F) in assemblages at and below this depth support the age assignment. This genus is restricted to the Santonian–Turonian interval.

Turonian sediments are recorded from 9200 ft (2804.2 m), this interval is below the FO of *Micula staurophora* (N) and supported by the FDO of *Praeglobotruncana* spp. (F). The base of the Middle Turonian is marked by FOs of both *Marthasterites furcatus* and *Eiffellithus eximius* (N) at 9400 ft (2865.1 m). The Upper Cenomanian is penetrated at 9790 ft (2984.0 m) characterized by the LO of *Axopodorhabdus albianus* and *Gartnerago praeobliquum* (N). Between 9820 and 9890 ft (2993.1–3014.5 m) the cuttings are dominated by Upper Turonian cavings, no *in situ* assemblages are recovered. Penetration of Middle–Lower Cenomanian is confirmed by the LOs of *Gartnerago theta* and *G. nanum* (N) at 9920 ft (3023.6 m). The oldest sample from 9950 ft (3032.5 m) yields *Corollithion kennedyi*, abundant *Broinsonia enormis* and *G. nanum* (N), confirming Cenomanian sediments; Upper Albian deposits are absent.

Three samples from the sandstones overlying the volcanics were analysed for palynology (3072.4–3288.8 m: Fig. 4); however, the samples were dominated by Late Cenomanian cavings.

Demerara A2-1

A2-1 was spudded by Esso in 1977 in 3937 ft (1200 m) water depth to appraise a large anticlinal structure over the Demerara Rise, offshore Suriname. The well was drilled to a total measured depth of 16 207 ft (4940.0 m) within previously reported Middle Jurassic (Callovian) platform carbonates and abandoned as a dry well, probably failing due to a lack of hydrocarbon charge. The lowermost *c.* 2350 m of stratigraphy in well A2-1 is composed mainly of an alternating limestone–mudstone sequence (Fig. 5). Limestone-dominated strata sharply decrease the GR log, forming distinctive blocky responses (Fig. 5); these sequences are up to 450 m thick. Petrographical analysis of these limestones reveals a mixture of microfacies within the cuttings; biomicritic, bioclastic, sandy and silty limestones are observed with a mudstone to grainstone texture, occasionally dolomitized. Limestones rich in bioclastic material contain fragments of ostracods, crinoids, spores, echinoid spines, recrystallized bivalve shells and framboidal pyrite, representative of platform carbonates. The microfauna include planktonic foraminifera observed in most limestone cuttings, with common cysts and spores, and occasional calpionellids (discussed below). Two samples from near TD of the well contain more argillaceous and siliciclastic material with minor organic matter. Sedimentation rates are relatively high, averaging 65.8 m Ma^{-1} throughout this interval (Fig. 2). This sequence is more mudstone-dominated towards the top, becoming increasingly organic (maximum TOC of 1.09%).

A 40 m-thick sandstone unit with remarkably similar lithological characteristics to the fine-grained sands in FG2-1 overlies this package and is interpreted as part of the Starbroek Formation (see Fig. S1 of the Supplementary material). Of note is the presence of glauconite, indicative of deposition in shallow-marine conditions (e.g. Stonecipher 1999) (see Fig. S1 of the Supplementary material), and the sedimentation rates. Limestones (Potoco Formation), 80 m thick, overlie these sands and are the first transgressive deposits above the BAU. The overlying unit is marked by a sharp increase in the GR log. A thick interval of calcareous mudstone with a high organic content is encountered that is eventually truncated by the BTU.

Dating

The youngest samples analysed at 7020 ft (2139.7 m) yielded a middle Campanian assemblage characterized by *Eiffelithus eximius*, *Uniplanarius sissinghi* and *Arkhangelskiellla cymbiformis* (N), and FDOs of *Contusotruncana fornicata*, *C. ?contusa* and *Rugotruncana subcircumnodifer* (F). The Middle Campanian Unconformity (MCU) is recognized in this well at 2156.65 m, with the underlying sediments recorded from 7110 ft (2167.1 m) yielding Santonian fauna characterized by *Marthasterites furcatus* and *Lithastrinus grillii* (N) below FOs of the *Broinsonia parca* group and *A. cymbiformis* (N). Organic mudstones of Coniacian–?Upper Turonian age are recovered over the interval 7260–7290 ft (2212.8–2222.0 m). The assemblages are characterized by *Quadrum gartneri*, *Eprolithus floralis* and *Lithastrinus septenarius* (N). The FO of *Micula staurophora* (N) at 7290 ft (2212.8 m: if *in situ*) would indicate an age no older than Coniacian. The occurrence of abundant *M. furcatus* (N) also at 7290 ft (2212.8 m) confirms an age no older than uppermost Turonian.

A relatively expanded Lower Turonian succession between 7410 and 7650 ft (2258.6–2331.7 m) is characterized by the high relative abundance (HRA) of *Eprolithus* spp. (N), including quantitative influxes of *Eprolithus moratus* and *E. floralis* (N) below the FO of *Eiffelithus eximius* (N). The LO of *Zeugrhabdotus scutula* ssp. *turonicus* (N) is at 7500 ft (2286.0 m), whilst the FO of *Quadrum gartneri* (N) is at 7590 ft (2313.4 m). The age assignment is supported by FDOs of *Whiteinella aprica* and ?*W. inornata* (F). Penetration of Upper Cenomanian strata is confirmed by the LOs of *Axopodorhabdus albianus*, *Gartnerago praeobliquum* and *Helenea chiastia* co-occurring with *Gartnerago obliquum* (N) at 7710 ft (2350.0 m). Lower Cenomanian age is penetrated at 7800 ft (2377.4 m) with the LOs of *Gartnerago nanum* and *G. theta* (N); the age assignment is supported by the LO of consistent *Eiffellithus paragogus* at 7840 ft (2389.63 m). The basal Cenomanian is characterized by the *Broinsonia plexus*, including *B. cenomanicus*, *B. signata* and *B. enormis* (N). Other characteristic nannofloral events of the basal Cenomanian are the HRA of *Helicolithus*

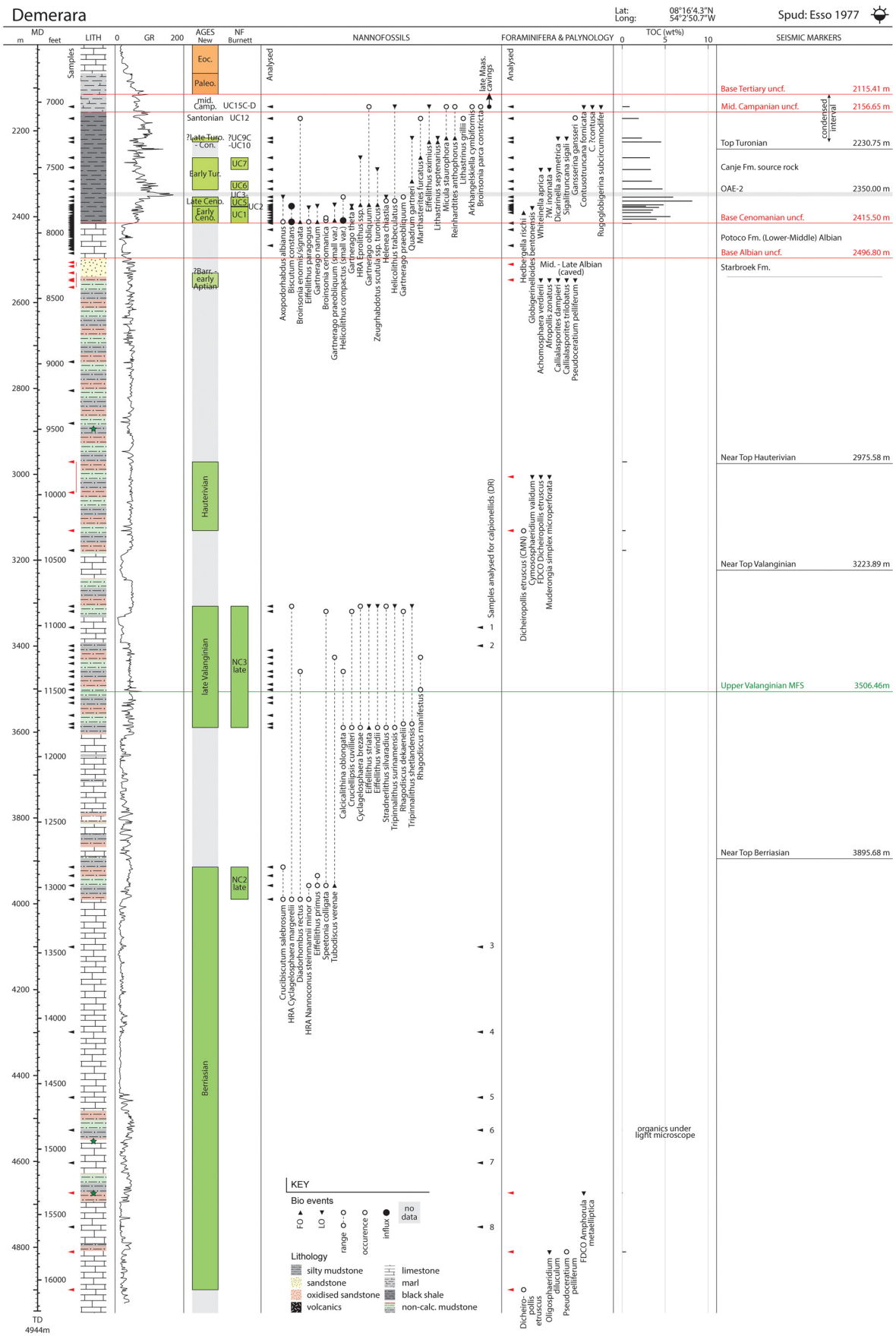

Fig. 5. A re-evaluation of the Demerara A2-1 well stratigraphy displaying nannofossil events (Table S2 of the Supplementary material), foraminifera and palynology results, total organic carbon (TOC: Table S1 of the Supplementary material) measurements, and key stratigraphic surfaces. Oil shows are indicated in the lithology column as green stars. Palynology abbreviations: CMN, common; FDCO, first downhole common occurrence. The location is displayed in Figure 1a.

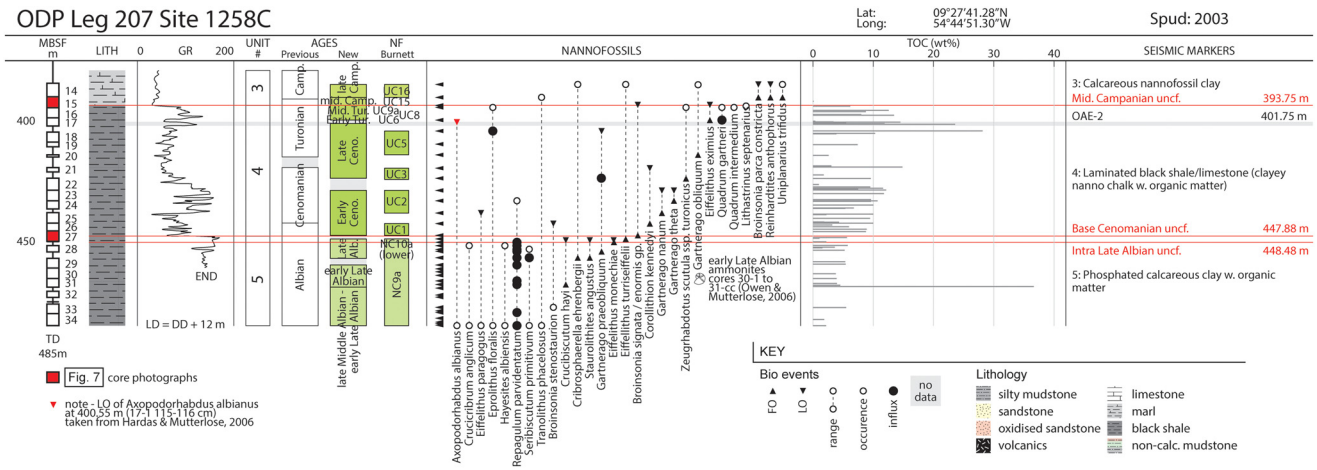

Fig. 6. A re-evaluation of the ODP Leg 207 Site 1258C stratigraphy displaying nannofossil events (Table S2 of the Supplementary material), total organic carbon (TOC: Table S1 of the Supplementary material) data compiled from Meyers *et al.* (2006) and key stratigraphic surfaces. A 12 m correction has been applied to the gamma-ray (GR) log, where LD is logger's depth and DD is driller's depth. Early Late Albian ammonites identified in cores 30 and 31 by Owen and Mutterlose (2006) are annotated, as well as the cores displayed in Figure 7. The location is displayed in Figure 1a.

compactus, *H. compactus* (small var.) and *Gartnerago praeobliquum* (small var.). At well A2-1, the Base Cenomanian Unconformity (BCU) lies directly upon a ?Lower Albian Potoco carbonate succession; no Upper–Middle Albian is preserved, as at ODP Leg 207 (Erbacher *et al.* 2004*a*).

The mudstone-dominated sequence below the BAU at 2496.4 m yields an intra-early Aptian–?Barremian marine dinocyst assemblage due to the presence of *Pseudoceratium pelliferum* (Duxbury 1983), *Achomosphaera verdierii* (Below 1982) and *Afropollis zonatus* (Doyle *et al.* 1982; P). The co-occurrence of common *Dicheiropollis etruscus* is a sporomorph event that has been recorded from unpublished data of Atlantic offshore Morocco within Hauterivian-dated sediments. It is widely recorded from undifferentiated Neocomian sediments offshore West Africa) and *Muderongia simplex microperforata* (Davey 1982; Costa and Davey 1992; P).

Between 10 840 and 11 790 ft (3307.1–3593.6 m) rich nannofloras yielding *Eiffellithus windii*, *E. striatus*, *Stradnerlithus silvaradius*, *Rhagodiscus dekaenelii*, *R. manifestus, Speetonia colligata*, *Cruciellipsis cuvillieri*, abundant *Cyclagelosphaera margerelii*, *C. brezae*, *Tubodiscus verenae* and *Tripinnalithus surinamensis* (N) are encountered, indicating penetration of late Valanginian sediments. Sporadic occurrences of *Calcicalathina oblongata* and *Diadorhombus rectus* (N) are also recorded. Nannoconids are dominated by the wide canal species *N. kamptneri*, *N. wassalii* and *N. cornuta* (N). The late Valanginian appears to record the Lower Cretaceous maximum sea level pre-Albian and associated increase in nannofloral diversity. This level is calibrated to the Upper Valanginian maximum flooding surface (MFS) (VF), an event recorded in this study from the Gulf of Mexico (Loucks *et al.* 2017; J. Jeremiah pers. obs.).

Below 11 790ft (3593.6 m) nannofossil diversity decreases with the increased frequency of platform limestones. A brief flooding event is recorded between 12 850 and 13 090 ft (3916.7–3989.8 m), where calcareous mudstones are encountered again. The nannoflora is characterized by *Crucibiscutum salebrosum*, *Nannoconus steinmannii minor*, *Diadorhombus rectus*, *Eiffellithus primus and Tubodiscus verenae* below the FO of *Calcicalithina oblongata* (N), an indication that late Berriasian sediments have been penetrated.

The current biostratigraphy study confirms the age at TD of this well as no older than late Tithonian based on calpionellid occurrences, much younger than previous studies that indicate an age as old as Callovian (Griffith 2017). The majority of the carbonate succession is of Early Cretaceous age. At 14 100 ft (4297.7 m) the top occurrence of *Crassicollaria intermedia* (C) is recorded, indicating that the late Tithonian has been penetrated, specifically the *Crassicollaria* Zone (Remane 1985; Blau and Grün 1997). Below this, the top occurrence of *Calpionella alpina* and *Crassicollaria parvula* (C) occurs at 15 100 ft (4602.5 m), as well as occurrences of *Calpionella alpina*, *Crassicollaria intermedia* and *Tintinnopsella carpathica* (C) at 15 590 ft (4751.8 m), which again are characteristic of the late Tithonian *Crassicollaria* Zone. The acme of *Calpionella alpina*, diagnostic of the Jurassic–Cretaceous boundary (Michalík and Reháková 2011; Wimbledon *et al.* 2011), is not recorded, probably due to the studied sampling interval, and therefore a tentative top Jurassic is placed at 4277.1 m. Three samples from the interval 15 330–16 070 ft (4672.6–4898.1 m) yield a low-diversity dinocyst assemblage of *Amphorula metaelliptica* (Dodekova 1969; Habib and Drugg 1983; van Helden 1986; Monteil 1992), *Oligosphaeridium diluculum* (Davey 1982) and *Pseudoceratium pelliferum* (P), indicating an age no older than Berriasian; the assemblage is considered caved.

ODP Leg 207

The following lithological summary is provided for the Cretaceous sediments of Site 1258C (the main focus of the study); however, a more complete description of the stratigraphy penetrated on Leg 207 and specifically Site 1258 is presented in Erbacher *et al.* (2004*a*, *b*) (Fig. 6). Additional data are presented from sites 1257A and 1260A. Cores from three Cretaceous units were recovered (Fig. 7): Unit 3, calcareous nannofossil clay (139 m); Unit 4, laminated black shale and limestone (55 m); and Unit 5, phosphoritic calcareous clay with organic matter (thickness 37 m). The top of Unit 3 is marked by 2 cm-thick layer of graded fine- to medium-sized green spherules representing the ejecta layer of the Cretaceous–Tertiary (K/T) boundary (Erbacher *et al.* 2004*a*, *b*). The uppermost section of Unit 5, Core 27 (Fig. 7) is calcified and indurated, which is interpreted to be indicative of multiple unconformities, hiatus and condensation, supported by low sedimentation rates (<5 m Ma^{-1}: Fig. 2).

Dating

All dates have been determined from calcareous nannofossil analysis (N). At Site 1258C, Erbacher *et al.* (2004*b*) described a Campanian unconformity, with the early Campanian–Santonian absent. This MCU is confirmed at the base of Core 15 -3 (Fig. 7), middle Campanian chalks yielding *Eiffelithus eximius*, *Broinsonia enormis*, *Broinsonia parca constricta* and *Arkhangelskilella cymbiformis* immediately above a condensed Middle Turonian

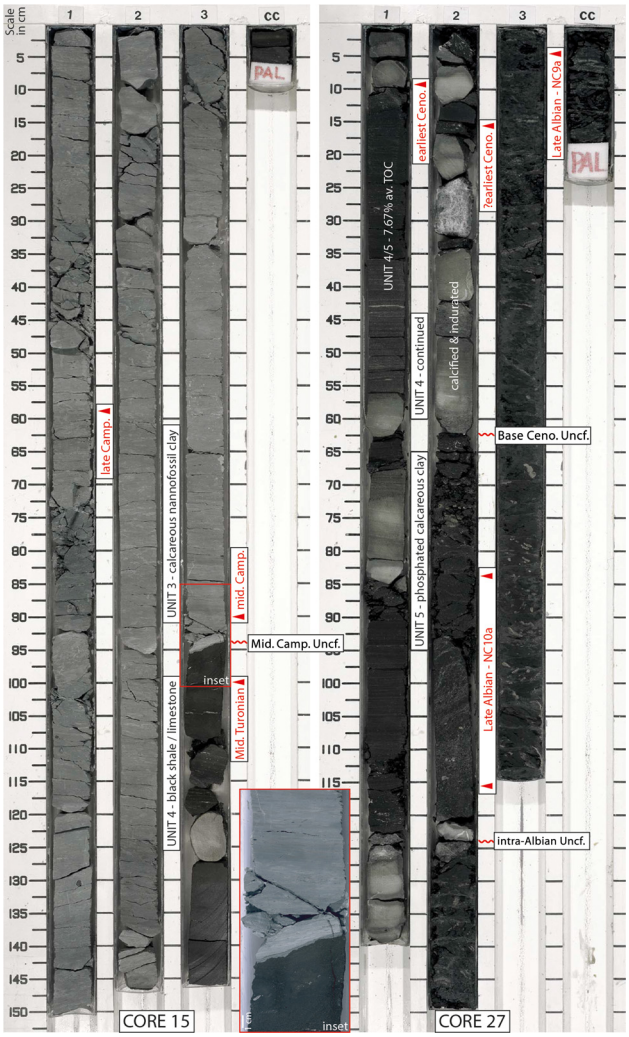

Fig. 7. Photographs of two cores, 15 and 27, from ODP Leg 207 Site 1258C with analysed samples and interpreted ages displayed by red arrows, highlighting the Cretaceous stratigraphy and unconformities present in the borehole (Erbacher *et al.* 2004*a*). Inset: zoom-in on the sharp contact between the calcareous nannofossil clay of Unit 3 and the black shale of Unit 4 representing the Middle Campanian Unconformity (MCU) and a *c.* 12 myr hiatus (Erbacher *et al.* 2004*b*). Ceno., Cenomanian; Camp., Campanian. The scale is in centimetres.

organic shale succession with *Quadrum gartneri* and *Lithastrinus septenarius* recorded at 393.77 m. Erbacher *et al.* (2004*a*) documented younger Coniacian organic mudstones preserved beneath the unconformity southeastwards at Site 1260. This is supported by sediments as young as Santonian age preserved beneath the MCU at well A2-1 (Fig. 5).

Hardas and Mutterlose (2006) investigated the Cenomanian–Turonian boundary from Site 1258C and recorded the LO of the Cenomanian marker, *Axopodorhabdus albianus*, at 400.55 m. Due to a sample gap, penetration of Cenomanian strata is confirmed slightly lower in the current study at 404.30 m; the LOs of *Axopodorhabdus albianus* and *Gartnerago praeobliquum* are recorded.

Lower Cenomanian sediments are proven at 428.95 m with the occurrence of common *Gartnerago theta,* the age assignment supported by the LO of consistent *Eiffellithus paragogus* at 438.32 m. Cenomanian strata are confirmed down to 447.58 m at Site 1258C with the FO of *Corollithion kennedyi*. Erbacher *et al.* (2004*b*) documented a major hiatus at the base Cenomanian with no support for the preservation of Upper Albian sediments. The current study supports the identification of the BCU, with latest Albian sediments missing. The upper part of Zone NC10 is not recorded. Intra-Late Albian-aged sediment is, however, recorded immediately below at 449.74 m with the LO of an increase in *Eiffellithus monechiae*; *E. turriseiffelii*, however, is still quantitatively dominant over *E. monechiae*, down to 450.06 m.

The FO of *E. turriseiffelii* and associated *E. monechiae* acme and earlier FOs are not preserved in 1258C. Another hiatus, an intra-Late Albian unconformity, is recorded from the base of Core 27-2 at 450.16 m; sediments occurring below are characterized by *Staurolithites angustus* at 450.45 m. The LOs of *Watznaueria britannica* and *Hayesites albiensis* are both recorded from 450.45 m, these forms are utilized as alternative top Albian markers (Watkins and Bowdler 1984; Burnett 1998); their LOs here depressed stratigraphically but of potential local correlative significance. Another major change in nannoflora at this stratigraphical level is the increase downhole of cold-water nannofossils such as the HRA of *Repagulum parvidentatum* below 450.45 m and consistent *Seribiscutum primitivum* below 451.85 m; events also recorded by Kulhanek and Wise (2006).

The oldest definitive Late Albian sediments at Site 1258C are confirmed by the FO of *Staurolithites angustus* and consistent *Cribrosphaerella ehrenbergii* (Jeremiah 1996, 2001; Bown 2001) at 456.84 m (Core 29-1). In addition, an assemblage of ammonites collected and examined by Owen and Mutterlose (2006) from cores 30 and 31, Site 1258C refine this age assignment to early Late Albian within the *Hysteroceras varicosum* Zone. Late Albian sediments are potentially confirmed as deep as 467.94 m with the FO of *Crucibiscutum hayi* (Jeremiah 1996; Bown 2001; Gale *et al.* 2011); similar forms, though, are known to range down into the Middle Albian (Jeremiah 1996). Hence, in the current paper these are assigned the age range of Middle–Late Albian.

Kulhanek and Wise (2006) also recorded *Eiffelithus monechiae* consistently down to Core 33-2, *Cribrosphaerella eherenbergii* almost to the base of the cored section at Core 34-2, and the boreal Upper Albian marker *Tegulalithus tessellatus* between cores 33-2 and 34-2. All of these markers are Upper Albian restricted but could not be corroborated in the current study at these deeper levels within the core. The interval 459.85–484.82 m yields an early Late Albian–late Middle Albian nannoflora. Boreal markers that would enable further subdivision of the early Late Albian–Middle Albian succession, such as *Tegulalithus tessellatus*, the *Ceratolithina plexus* and *Braloweria boletiformis*, are all absent. The consistent occurrence of *Axopodorhabdus albianus* to the base of the cored section at 484.82 m, however, confirms an age no older than late Middle Albian.

Sporadic records of *Axopodorhabdus albianus* are recorded from the lower Middle Albian (Jeremiah 1996, 2001; Bown 2001; this study DSDP Site 144 299.28 m). Base consistent *A. albianus* from the upper Middle Albian was preferred by Jeremiah (1996, 2001; Bown 2001) as a cosmopolitan event, and supported by observations from Texas by Hill (1976) and Bralower *et al.* (1993).

The oldest cored sediments investigated from the Demerara Rise on ODP Leg 207 were found at sites 1257A and 1260A. Here, early Middle Albian nannofloral assemblages were recovered similar to that recorded from DSDP Leg 14 Site 144 (Table S2 of the Supplementary material).

DSDP Leg 14 Site 144

The objective of DSDP Leg 14 Site 144 was to recover the oldest marine sediments of the proto-Atlantic (Hayes *et al.* 1972). Three boreholes (A, B and Z) were drilled to a TD of 327 m, recovering 10 cores, totalling 31.9 m in length, from four Cretaceous-aged units (Fig. 8): Unit 2, zeolitic greenish-grey marl; Unit 3, black and olive zeolitic marl; Unit 4, olive green marl; and Unit 5, silty quartzose

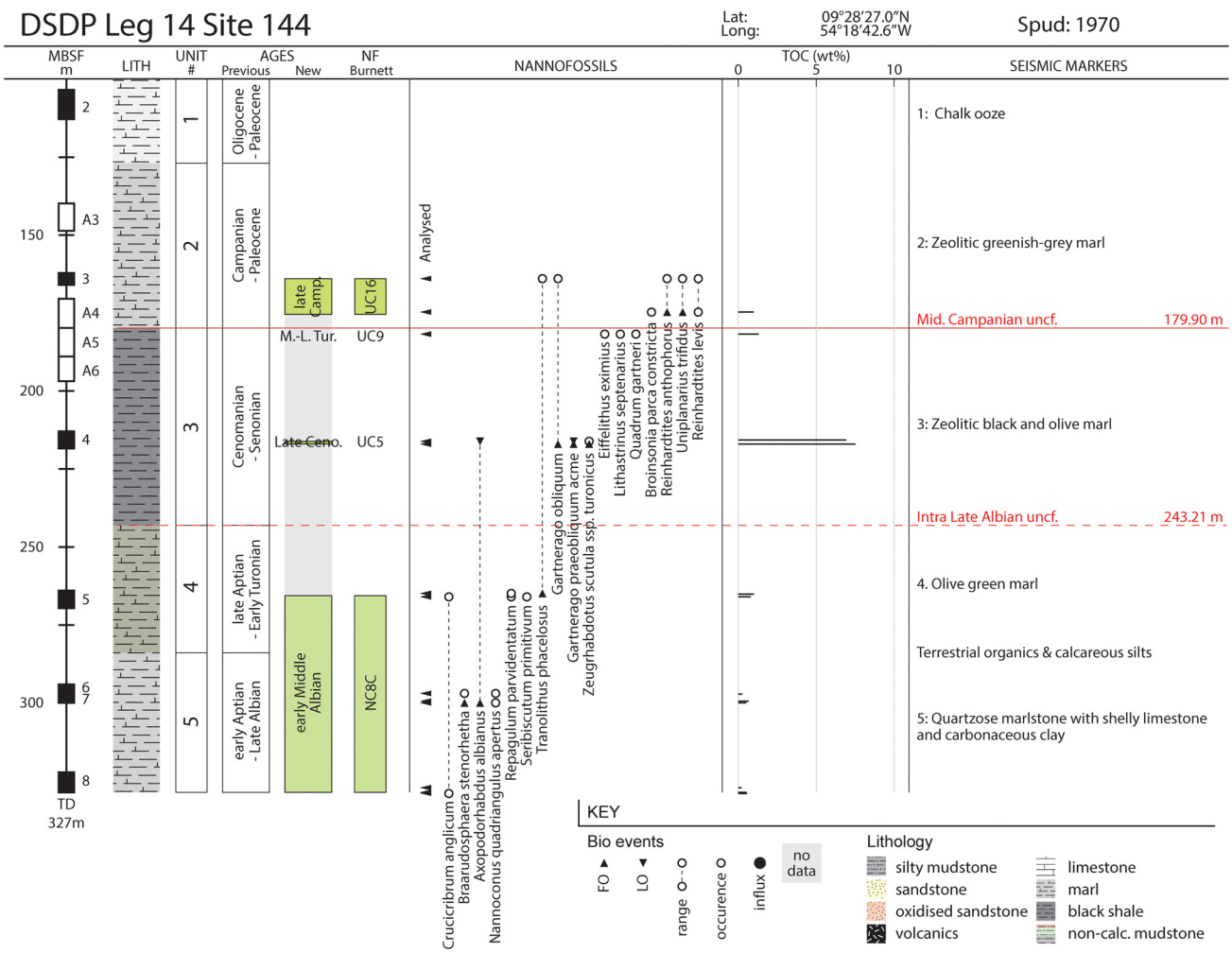

Fig. 8. A re-evaluation of the DSDP Leg 14 Site 144 stratigraphy displaying nannofossil events (Table S2 of the Supplementary material), total organic carbon (TOC: Table S1 of the Supplementary material) measurements and key stratigraphic surfaces. The location is displayed in Figure 1a.

marl with shelly limestones and background organics. These units differ from the lithostratigraphic units of ODP Leg 207 (Figs 6 and 7).

Dating

All of the age datings are determined from calcareous nannofossil analysis (N). The hiatus associated with the MCU is also recorded at DSDP 144 where late Campanian sediments from the base of Core 4-2 (173.96 m) are recorded only 7 m above Middle–Upper Turonian sediments at the top of Core 5-1 (Fig. 8). The sample at 181.05 m yields *Eiffellithus eximius* and *Quadrum gartneri* below the FO of *Micula staurophora*. Upper-Cenomanian-aged sediments yielding *Gartnerago obliquum*, *G. praeobliquum* and *Axopodorhabdus albianus* are recorded from cores 4-2 to 4-3 (Fig. 8), equivalent to Core 19-1 at ODP Site 1258C (Fig. 6). An early Middle Albian succession is preserved in the interval 264.14–328.35 m (TD). The base Middle Albian age assignment is supported by the FO of *Tranolithus phacelosus* at 264.14 m and the absence of consistent *Axopodorhabdus albianus*. A Middle Albian age to the base of the cored section is supported by the presence of *Crucicribrum anglicum* down to 328.35 m. *Braarudosphaera* spp. are recovered including *B. stenorhetha*, in association with nannoconids including *Nannoconus quadriangulus quadriangulus* and *N. q. apertus*.

Organic geochemistry

Combined with re-dating of sediments from the seven wells and scientific boreholes studied, further organic geochemical analysis was undertaken to improve characterization of the prolific Upper Cretaceous organic-rich interval (Canje Formation) encountered along the continental margin. This source rock in the basin kitchens either side of the Demerara Rise (Fig. 1a) has been generating hydrocarbons from the Late Miocene to present day (James *et al.* 2020). Hydrocarbons charge turbidite reservoirs in the base-of-slope to basin-floor setting in the Guyana–Suriname Basin (Cedeño *et al.* 2019) and offshore French Guiana, observed in the GM-ES-1 well, and through long-distance migration to the onshore Tambaredjo heavy oil field in Suriname (Fig. 1a) (Dronkert and Wong 1993). In addition, the new dataset improves our understanding of older source potential (i.e. Jurassic).

The new data generated from DSDP Site 144 and ODP Site 1258C refines the onset of organic-rich sedimentation on the Demerara Rise to occur during the late Middle Albian. Early Middle Albian olive green marls from DSDP Site 144 (and ODP Sites 1257A and 1260A) are organic-lean, with average TOC from cores 5–8 at 0.65% (Fig. 8); whereas late Middle Albian black shales recovered from ODP Site 1258C average 4.23% TOC (Figs 6 and 7). Pyrolysis reveals that the organic matter is Type II algal material (Unit 4) and mixed Type II/III (Unit 5: Erbacher *et al.* 2004*b*).

Throughout the wells, TOC values peak around the Cenomanian–Turonian boundary (approximating to OAE-2), reaching a maximum value at ODP Site 1258C of 28.13% TOC, as recorded globally (Schlanger *et al.* 1987). This peak is observed in additional exploration wells on the Guyana Shelf (AR-1 and ESS-2) (Mourlot 2018), and is commonly associated with a significant peak in the GR log (Figs 4 and 5). This peak is subdued in GM-ES-3 (Fig. 3),

probably due to the proximity of sand-dominated turbidite systems suppressing the signature. In all of the wells studied on the Demerara Rise, the Upper Cretaceous organic-rich interval is truncated by the MCU. Campanian organic content is present in FG2-1, documented to be terrestrially-derived (Fig. 9). Average TOC values for the Canje Formation vary along the margin; on the Demerara Rise the highest average TOC values are recorded on the northwestern distal margin at DSDP Site 144 (7.22%) and ODP Site 1258C (7.67%). The TOC decreases towards the palaeocoastline in A2-1 to 3.96%, and again at FG2-1 to 2.09%. In the Equatorial Atlantic domain at GM-ES-3 TOC averages 4.28%.

Source-rock maturity indicated by T_{max} values range from 346 to 430°C, averaging 418°C, indicating that all samples are immature (Table S1 of the Supplementary material). To compare source-rock quality and kerogen type, hydrogen and oxygen indices were plotted on a modified van Krevelen diagram (Fig. 9). Raw data are presented in Table S1 of the Supplementary material. To understand temporal changes in kerogen type, the symbology reflects the age of the sample. The majority of samples have a high hydrogen index (HI: 475–600+ mgHC g^{-1} organic carbon) and low oxygen index (OI: 20–65 $mgCO_2$ g^{-1} organic carbon) indicating Type II marine kerogen with oil-generating potential. Outliers from this group with low HI and high OI values are all early Middle Albian in age from DSDP Site 144 (cores 5–8) indicative of gas-prone Type III terrestrial kerogen. Younger Albian samples show a progressive increase in HI and decrease in OI towards the Type II group, indicating the gradual increase in marine-type organic matter through this interval. Cenomanian–Coniacian samples from FG2-1 have lower HI and higher OI values (average HI, 251 mgHC g^{-1} organic carbon; average OI, 76 $mgCO_2$ g^{-1} organic carbon) showing a mixing between Type II/III. This reflects the relative position of FG2-1 closer to the palaeoshoreline and sediment input from river systems, and therefore likely to receive more terrestrial input as indicated by the higher sedimentation rates compared to the time-equivalent interval in A2-1 (Fig. 2). Pyrolysis results from GM-ES-3 fall within a tight grouping away from main Type II signature with low OI (20–30 $mgCO_2$ g^{-1} organic carbon) and moderate HI (200–450 mgHC g^{-1} organic carbon) values, suggesting a mixing of kerogen types. S_1 peaks are representative of hydrocarbons generated at low temperatures during the pyrolysis and indicate free or absorbed hydrocarbons (Allen and Allen 2013). Average S_1 values for GM-ES-3 samples are 21.4 mg g^{-1}, compared to an average of 1.0 mg g^{-1} for all remaining samples, indicating free hydrocarbons throughout the interval analysed in GM-ES-3. Alongside the low T_{max} values (immature), this suggests that the free hydrocarbons are migratory.

Geochemical analysis of samples below the BAU in A2-1 (i.e. Aptian–Berriasian) all yield low TOC values (average 0.37%). Higher values of 1.1–1.5% TOC were previously reported by Griffith (2017) from this interval as indicative of a Middle Jurassic (Callovian) synrift source rock based on the original biostratigraphy. Our new age dating proves that no Callovian sediments were encountered in A2-1, meaning the well did not penetrate a synrift source rock below the Demerara Rise. However, this new evidence does not rule out the potential for a Jurassic source rock along the margin. Seismic evidence from this study supports the interpretation of additional older Jurassic sediments below the well TD of A2-1, distributed deeper across the Demerara Rise (see the following subsection 'Margin Architecture') and onto the Guinea Plateau. Oil and gas shows within the Lower Cretaceous interval are reported, suggesting deeper source-rock potential as the main organic-rich interval sits above the BAU (Fig. 5). Additional support for a potential Jurassic source rock is evidenced by proven Jurassic-aged lacustrine shales with 2.5% TOC within the Takutu Graben onshore (Webster 2004), and predicted from gravity data in two graben

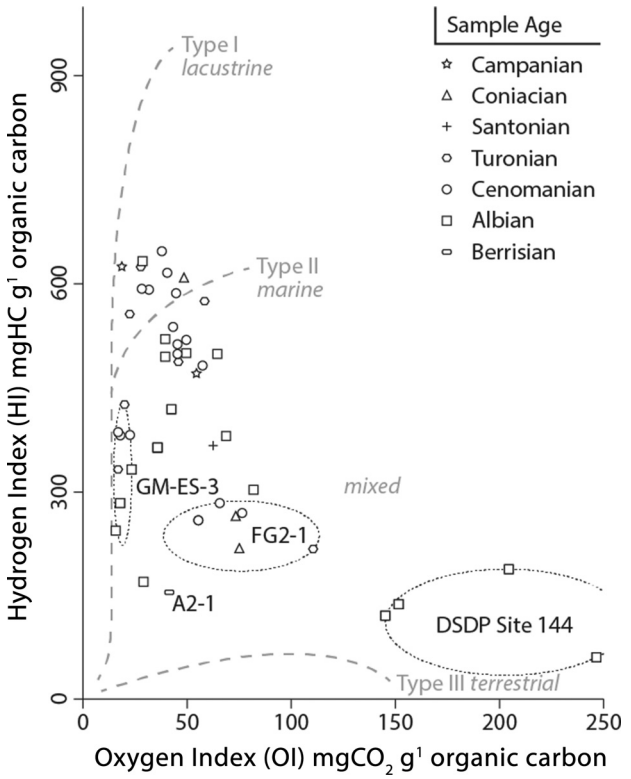

Fig. 9. Classification of kerogen types using hydrogen and oxygen indices plotted on a modified van Krevelen diagram displaying the results of the Rock-Eval pyrolysis. The symbology reflects the age of each sample analysed. New data generated in this study from four of the revised wells (A2-1, DSDP Site 144, FG2-1 and GM-ES-3) are amalgamated with data presented in Meyers *et al.* (2006) from ODP Site 1258C; the ages are updated following the new biostratigraphy results. The tabulated data are presented in Table S1 of the Supplementary material.

offshore (Nickerie and Commeqijine: Fig. 1b) (Griffith 2017). Further geochemical work by Cedeño *et al.* (2019) of oil recovered from wells onshore Suriname (Tambaredjo Field) revealed two hydrocarbon groups, one typed to the proven Upper Cretaceous source rock and another group from a source that generated hydrocarbons from terrestrial organic matter in marly sediments interpreted as Jurassic or Lower Cretaceous in age. These hydrocarbons are postulated to have been generated from the Lower Cretaceous interval penetrated by A2-1.

The hydrocarbons at the Liza and Tambaredjo fields have migrated out of the deep Guyana–Suriname Basin from the Canje Formation, sitting on oceanic crust (Fig. 1b) (Cedeño *et al.* 2019). We postulate that an unpenetrated early Aptian source rock (OAE-1A equivalent) may be present in the deep marine basin (Bihariesingh 2014), and absent across the Demerara Rise and basin margins. In addition, along the French Guiana margin, Aptian lacustrine synrift deposits may be potential source-rock candidates.

Hydrocarbons were extracted from four Lower Cretaceous–Upper Jurassic samples (well A2-1) with very low organic richness (0.11–0.43%) yielding very low quantities. It is difficult to determine for certain if the extracts are a naturally occurring product or a drilling-introduced contaminant. If the former, then their geochemical characteristics are very consistent and would most likely represent the residual product of migratory hydrocarbons rather than *in situ* generation. Overall, the extracted hydrocarbons are from an aquatic (possibly marine) environment but with significant terrestrial input (Fig. 9).

To summarize, further geochemical characterization of the main source rock (Canje Formation) reveals heterogeneities in the age of organic-rich sedimentation, organic richness and kerogen type. The

highest TOC with marine Type II kerogen occurs at the Cenomanian–Turonian boundary (OAE-2), typically recognized as a spike in the GR log profile. Free hydrocarbons are recorded throughout all of the samples analysed in GM-ES-3. Jurassic source potential is not encountered in A2-1; further evidence for its occurrence is postulated. Aptian source-rock potential is hypothesized.

Margin architecture

Mapping of the deep-penetrating GuyanaSPAN seismic data tied to the re-evaluated wells (Fig. 10) reveals the seismic–stratigraphic architecture of the Guyanas continental margin (Figs 11, 12 and 13). Three Mesozoic megasequences are defined and discussed based on our new data (Fig. 2).

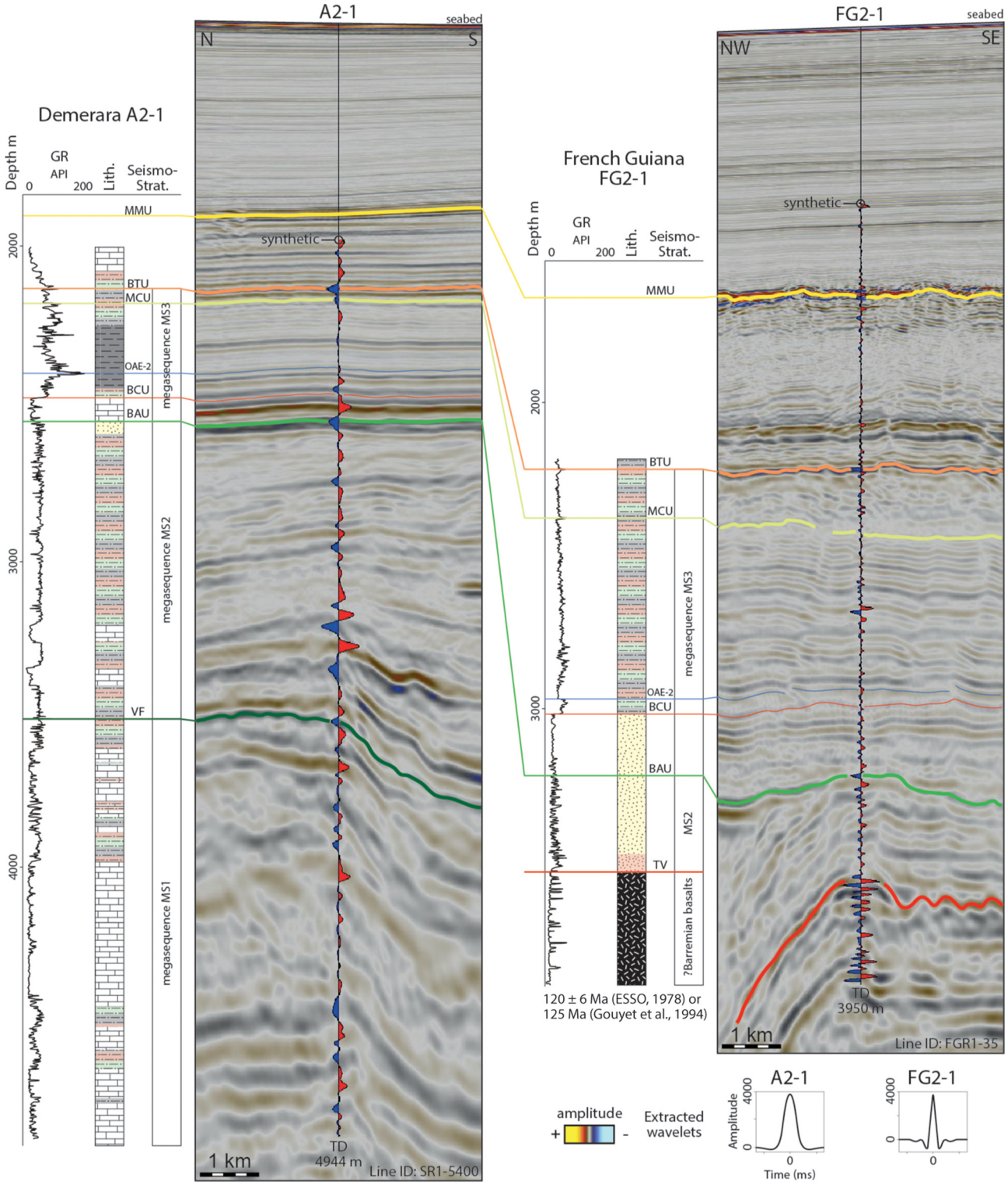

Fig. 10. Synthetic seismogram calculated for two exploration wells, Demerara A2-1 (Fig. 5) and French Guiana FG2-1 (Fig. 4), providing the well to seismic correlation of key horizons and megasequences identified in this new stratigraphic study. Extracted statistical wavelets are presented. The locations of the two wells are displayed in Figure 1a.

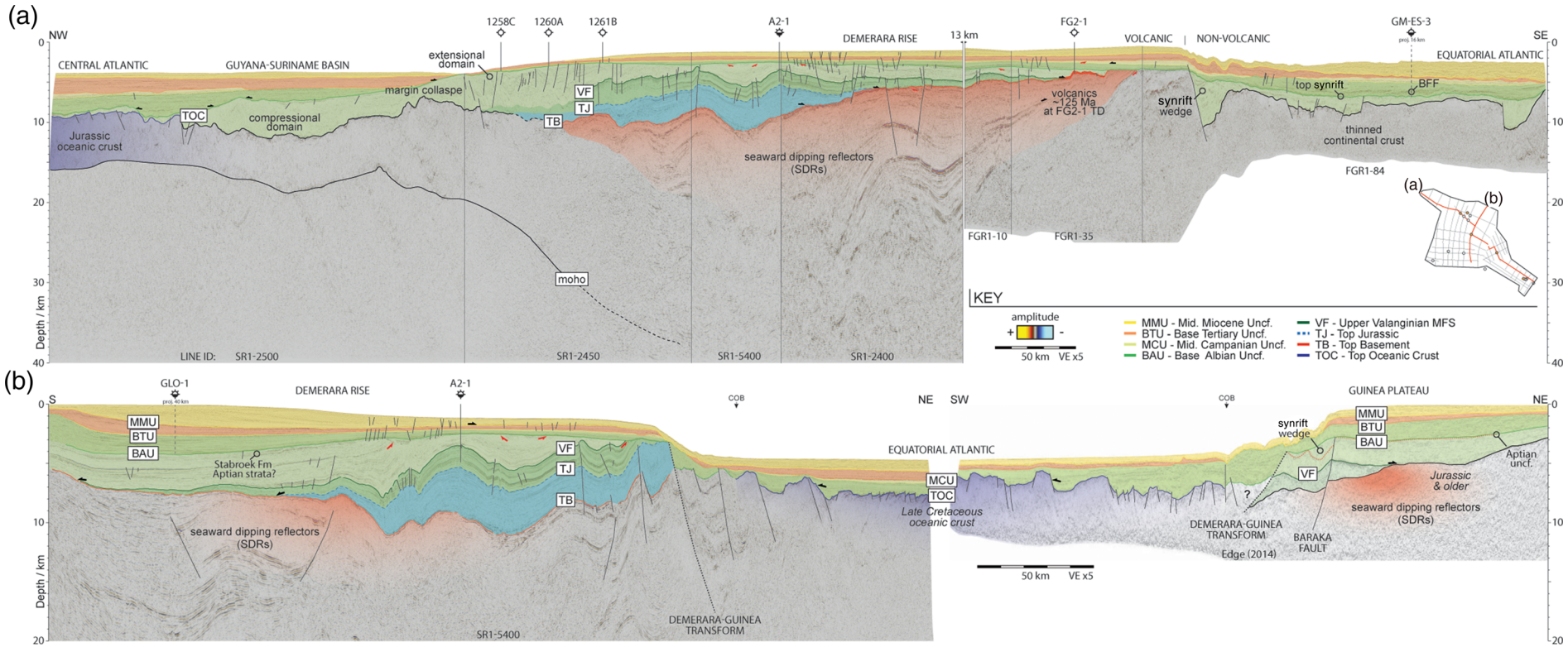

Fig. 11. (**a**) Composite seismic section in depth displaying megasequence architecture along a length of >1000 km of the Guyanas continental margin. The location is displayed in Figure 1a. Erosional truncation (red arrows) and onlap (black arrows) are marked. BFF, basin-floor fan; MFS, maximum flooding surface. (**b**) Conjugate dip-orientated seismic depth sections from the Demerara Rise (2D line: SR1-5400, clipped at 20 km depth) and Guinea Plateau (after Edge 2014) displaying megasequence architecture. The location is displayed in Figure 1a and the reconstructed location in Figure 16a. Note the change of the horizontal and vertical scale from (a). COB, continent–ocean boundary. Seismic data courtesy of ION Geophysical.

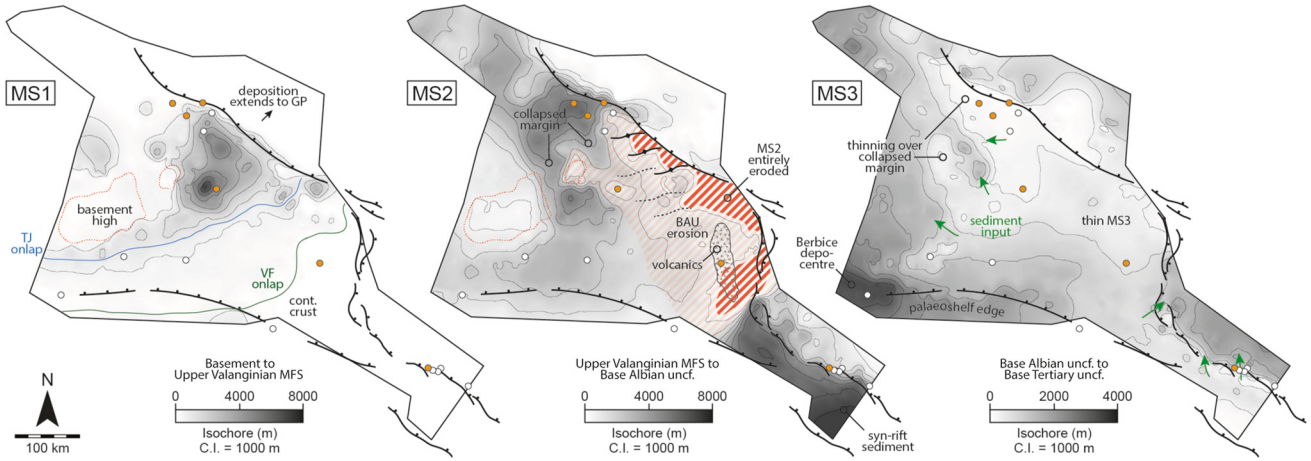

Fig. 12. Isochore thickness maps for three megasequences: MS1, top basement (SDRs, continental and oceanic crust) to upper Valanginian maximum flooding surface (VF); MS2, VF to Base Albian Unconformity (BAU); MS3, BAU to Base Tertiary Unconformity (BTU). Cont., continental; GP, Guinea Plateau; TJ, top Jurassic.

Basement

As introduced earlier, the 'basement' in this study is defined as the crust plus pre- and synrift sediments that exist below the Central Atlantic post-rift succession. Previous studies (Mercier de Lépinay *et al.* 2016; Reuber *et al.* 2016; Kusznir *et al.* 2018) have characterized this interval, which is beyond the scope of this paper. However, a brief overview is provided summarizing the evidence for the two models of basement composition. Despite the nature of the basement, the top surface is defined by a major unconformity, interpreted as the top basement (TB), with MS1 strata successively onlapping this surface towards to the southeast (Figs 12 and 13).

The main evidence for the volcanic nature of the basement below the Demerara Rise is the interpretation of SDRs based on deep-penetrating seismic data (Yang and Escalona 2011; Mercier de Lépinay *et al.* 2016; Reuber *et al.* 2016). Clearly, in Figure 11a, the basement comprises a series of high-amplitude reflections forming a thick package (up to 21 km), dipping towards the Guyana–Suriname Basin to the NW (i.e. seaward dipping). The interpreted basaltic flows have either been associated with the migrating Bahamas hotspot (Morgan 1983) during early opening of the Central Atlantic (*c.* 158 Ma: Reuber *et al.* 2016) or related to the Central Atlantic Magmatic Province (CAMP) volcanism (*c.* 200 Ma: Loncke *et al.* 2020). Volcanism is further supported by recovered dredge samples of Jurassic-aged (173.4 ± 1.6 Ma) rhyolites and basalts from the Demerara Rise (white star in Fig. 1a) (Basile *et al.* 2020). In addition, Zinecker and Mann (2020) report SDRs below the conjugate Guinea Plateau.

Megasequence 1 (MS1)

Well A2-1 penetrated the deepest and oldest stratigraphy on the Demerara Rise, redated as late Tithonian. This succession (up to

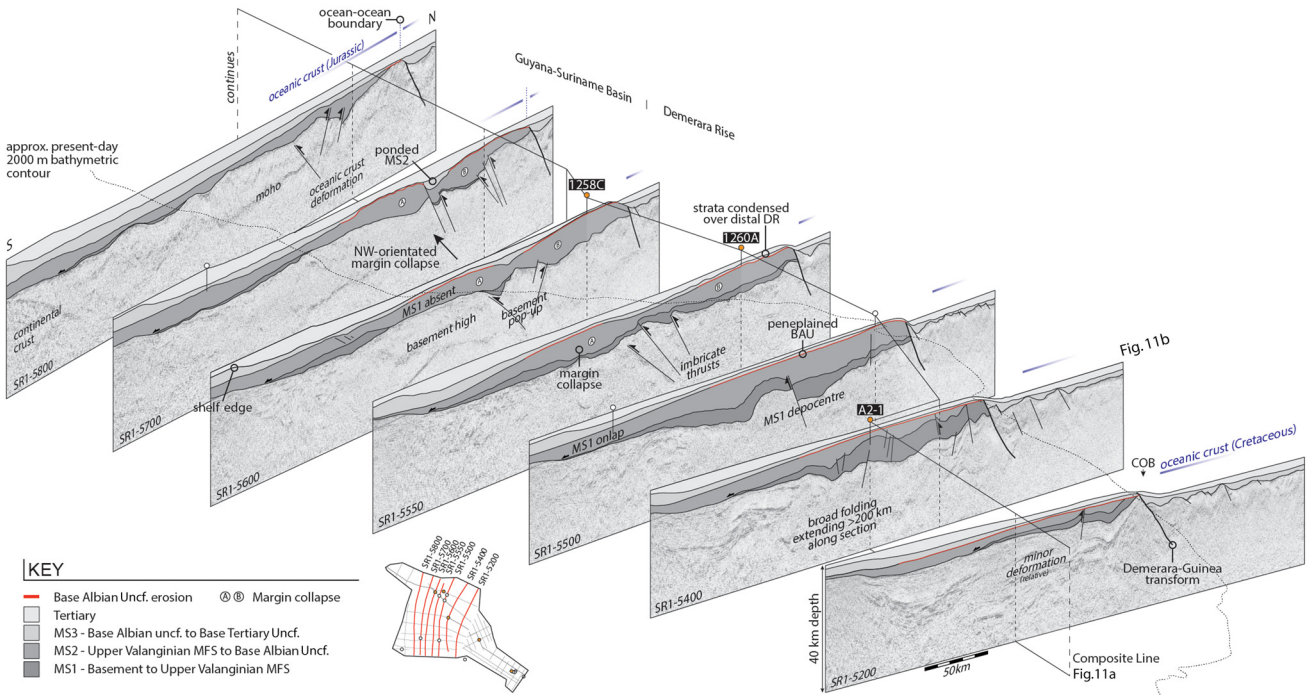

Fig. 13. A fence diagram constructed from seven dip-orientated (north–south) seismic depth sections across the Demerara Rise, interpreted with the megasequences, structural domains and underlying basement structure. BAU, Base Albian Unconformity; COB, continent–ocean boundary. Seismic data courtesy of ION Geophysical. The locations are shown in the inset.

7 km thick) of alternating limestone and mudstone forms parallel, high-amplitude reflections (limestones) interspersed with low-amplitude, transparent acoustic facies (mudstones) that are extremely laterally continuous (>200 km: Fig. 11a). MS1 and MS2 both prograde basinwards towards the NW. The upper Valanginian MFS (VF) encountered in A2-1 onlaps the TB in a more proximal position (near FG2-1), defining the southeastern limit of Central Atlantic Ocean during the Lower Cretaceous. The MS1 interval is thickest below A2-1, extending below ODP Leg 207 sites (Fig. 12), and temporally records the highest sedimentation rates from the studied wells (Fig. 2). Sediments thin over a series of NE-trending basement highs and thicken inboard to form an elongate depocentre aligned along the palaeoshelf edge. MS1 sediment is absent NE of the Guinea–Demerara transform on this map due to succeeding Equatorial Atlantic rifting (now located below the Guinea Plateau) and is notably thin to absent above Jurassic-aged oceanic crust in the Guyana–Suriname Basin (Figs 11a, 12 and 13).

Megasequence 2 (MS2)

The Valanginian flooding surface (VF) defines the base of MS2, which comprises a Hauterivian–Aptian-aged mudstone-dominated package, with the top truncated by the BAU across the distal area of the Demerara Rise (Fig. 13). MS2 shows gradual progradation (Fig. 11b) culminating in the major fluvio-deltaic system (Stabroek Formation). Mapping MS2 thickness shows that the sequence is completely eroded and peneplaned by the BAU to the north and east against the arcuate-shaped bounding faults of the Demerara Rise (Fig. 12). The pre-Albian NE-trending anticlinal folds appear to control the amount of erosion, suggesting that MS2 was deformed first, followed by peneplanation (Fig. 12). BAU erosion decreases towards the SW, highlighted along the dip profile (Fig. 11b) and fence diagram (Fig. 13). Towards the present-day South American coastline the sequences below the unconformity are less deformed and no truncation is observed, suggesting a more complete section and the BAU becoming a correlative conformity (Fig. 11b) (Mitchum and Vail 1977). On the northwestern margin of the Demerara Rise below the ODP Leg 207 sites, the pre-Albian sediments are rotated by extensional listric normal faults, and thin over a basement high showing compressional features (thrust faults) 100 km downdip in the Guyana–Suriname Basin (Fig. 11a). The extensional domain is divided from the remainder of the Demerara Rise by an arcuate fault zone defining the headwall, positioned above continental crust; the compressional domain is emplaced on Jurassic oceanic crust (Fig. 11a). This feature is interpreted as a major gravitational margin collapse and forms two thick NW-trending lobes with a spatial extent of over 1000 km^2 emplaced around the basement high (Fig. 13). These lobes (A and B) are observed in strike profile in Figure 13, separated by a thrusted basement high.

The BAU can be followed through the Guyana–Suriname Basin, where overlying sediments onlap this surface. MS2-aged sediments of the French Guiana margin show growth strata into a major basin-bounding eastward-dipping normal fault (Fig. 11a). The thickest MS2 deposits occur along this section of the margin, controlled by accommodation generated in a series of en echelon normal faults recording the synrift non-marine sediments of the proto-Equatorial Atlantic encountered at TD in GM-ES-3 (Fig. 12). These MS2 sequence synrift sediments attain maximum thickness in the Brazilian Cacipore graben: wells here penetrate >3000 m of non-marine clastics, seismic indicating that these rifts attain >6000 m thickness (J. Jeremiah, pers. obs.). At FG2-1, the basaltic lavas encountered at TD of the well are expressed in the seismic data as a chaotic high-amplitude package interpreted to pinch out to the NE and onlap the basement to the SE (Fig. 11a). Their distribution forms a north-trending elongate ribbon (Fig. 1b) (Gouyet *et al.* 1994) emplaced above thinned continental crust (Fig. 11a). These break-up volcanics within MS2 are interpreted to be emplaced during Equatorial Atlantic rifting.

Megasequence 3 (MS3)

The Late Albian–Maastrichtian MS3 sequence is highly condensed on the NW of the Demerara Rise, thickening inboard and outboard into the surrounding basins (Fig. 12). These sediments onlap the BAU and gravitational margin collapse, and passively infill the oceanic crust topography beyond the Demerara–Guinea transform in the Equatorial Atlantic (Fig. 12). The remnant topography generated by the gravitational margin collapse is the primary control for MS3 distribution in this area, forming a long-lived sediment depocentre between the two lobes of the gravitational collapse (Fig. 13). A thick depocentre is observed orientated east–west located in the south of the study area, related to the location of the palaeoshelf edge and major sediment input (20.5 Mt a^{-1}: Ugwu-Oju 2018) through the shelf-incised Berbice Canyon.

An unconformity truncates the stratigraphy in the middle of MS3 (MCU in Fig. 11). In the surrounding basins, erosive incisions at the MCU, hundreds of metres deep, cut into the underlying stratigraphy containing low-amplitude fill (Fig. 11a). These are interpreted as the laterally equivalent channel–lobe systems supplying reservoir sands to the recent hydrocarbon discoveries within the Late Cretaceous succession of the Guyana–Suriname Basin, and the Cingulata turbidite fan system in French Guiana. In contrast to the broad topographical relief of the Demerara Rise, the French Guiana margin is much steeper where sediment input is point-sourced at relay zones related to the underlying normal fault array (Fig. 12). The top of the Cretaceous (top MS3) is defined by the BTU across the study area. All of these unconformities are more pronounced on the distal area of the Demerara Rise (Fig. 11).

Structural evolution

Although the structural evolution of the Demerara Rise has been studied before (Gouyet 1988; Basile *et al.* 2013; Reuber *et al.* 2016), important new insights can be developed by employing the new stratigraphic results with deep-penetrating seismic sections to examine the deformation and basement structure along strike (Fig. 13). Sequential restoration by horizon flattening reveals the structural evolution of the continental margin (Fig. 14).

Angular onlap of the MS1 sequence onto the TB is apparent (Fig. 14d), suggesting that significant topography was present prior to deposition of MS1. Flattening on the TB shows that the basement was broadly folded prior to the establishment of the Central Atlantic Jurassic carbonate platform (Fig. 14d). Eventual flooding of the palaeotopography occurred in the upper Valanginian (Fig. 14d). A major depocentre is mapped in MS1 (Fig. 12) positioned above the youngest SDR sequence (syn-6 *sensu* Reuber *et al.* 2016) that is located between the Jurassic oceanic crust and the thinned continental crust, indicating the area of maximum subsidence. MS1 is therefore interpreted to represent fill of accommodation following the opening of the Central Atlantic.

The Aptian (125–113 Ma) onset of Equatorial Atlantic extension generated synrift sinistral en echelon half-graben along the divergent margin east of the Demerara Rise (Fig. 14c) (Pindell 1985; Greenroyd *et al.* 2007, 2008; Basile *et al.* 2013). On the Demerara Rise, the Equatorial Atlantic rifting induced a transpressional tectonic regime across the northern margin due to movement on the Demerara–Guinea transform. This induced compression buckling of the MS1 and MS2 stratigraphy into tight (wavelength 30–50 km) anticlinal folds trending ENE (Fig. 12). Major imbricate thrust-fault systems with hundreds of metres of displacement

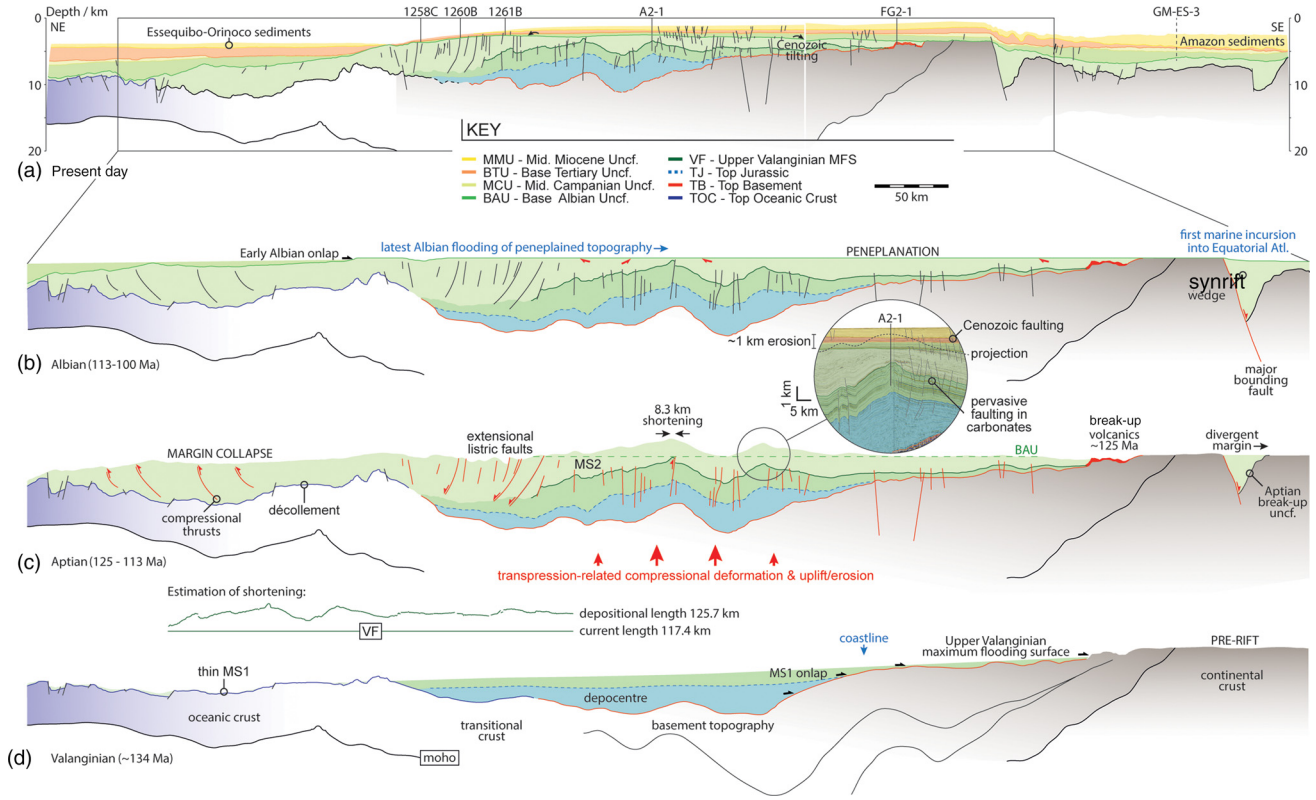

Fig. 14. Sequential restoration by horizon flattening for a segment of the strike seismic profile displayed in Figure 11a, at three key time stages: (**d**) Valanginian, (**c**) Aptian and (**b**) Albian revealing the structural evolution of the continental margin to (**a**) present day. A zoom-in on the seismic around Demerara A2-1 with a projection of the uppermost truncated seismic reflection (black dashed line) revealing *c.* 1 km of erosion at the well location is shown. MFS, maximum flooding surface. See Figure 1a for the location of the section.

contain associated rollovers and basement pop-up structures (Fig. 13). The orientation of these features indicates a maximum palaeostress direction orientated NW–SE, suggesting that there was significant compression associated with the transpressional Equatorial Atlantic break-up (Fig. 12b). Faulting also affects the underlying basement sequence and is pervasive in the rheologically competent carbonate lithologies. An approximate estimation of shortening by measuring the most continuous stratigraphic surface (VF) suggests 8.3 km of shortening along the profile orientated in the direction of maximum compression (Fig. 14c).

Maximum deformation and basin inversion occur localized above the thickest MS1 and MS2 deposits. Deformation continues outboard onto Jurassic oceanic crust (Fig. 13). At this time there is evidence for gravitational margin collapse to the NW into the Guyana–Suriname Basin induced by uplift-related instability. The compressional features, inversion and gravitational collapse of the margin are all related to transpressional deformation along the sheared northern margin of the Demerara Rise (Gouyet 1988).

The compression-related palaeotopography was subsequently peneplaned by the BAU across the full width of the Demerara Rise, truncating up to 1 km of section at the A2-1 well location (Fig. 14b), comparable to the amount of erosion observed in the megasequence isochore mapping (Fig. 12). There is a lack of any major incisional features on the peneplaned surface that would be indicative of canyon systems at the resolution of our dataset. The recognition of red oxidized sands in FG2-1 indicates subaerial exposure at this time. Erosion by a combination of subaerial (denudation) and shallow-marine submarine processes (wave action) created the peneplain architecture. Eroded sediments are postulated to have filled depocentres adjacent to the Demerara Rise. Accommodation generated by the major bounding fault on the eastern margin of the Demerara Rise forms a significant synrift wedge capped by the BAU (Fig. 11a), which is likely to have received some of the eroded material. Further deformation of the BAU results in the surface subtly tilted to the east and west (Fig. 14a). This deformation is related to the loading of adjacent oceanic crust by the initiation of the Amazon, Essequibo and Orinoco river systems in the Cenozoic, depositing excessively thick deep-sea fans, loading the crust and causing subsequent flexure of the Demerara Rise (Greenroyd *et al.* 2005; Basile *et al.* 2013).

Chronostratigraphic analysis

Visualization in the geological time domain of the stratigraphic architecture can be enhanced through the construction of a Wheeler diagram or chronostratigraphic chart, building a spatiotemporal stratigraphic framework (Wheeler 1958) (Fig. 15). Key stratigraphic surfaces and sequences, redated from the samples analysed from seven key wells and scientific boreholes, were used as the framework and later extended to an additional 13 exploration wells. The Wheeler diagram (Fig. 15) highlights the variability in the age and composition of the basement template as documented earlier. Several wells penetrate continental crust along the margin, with Arapaima-1 (AR-1) recovering phyllitic schists. The Jurassic–Barremian stratigraphy is restricted to below the Demerara Rise based on seismic interpretation (MS1 mapping: Fig. 12) and is only penetrated by A2-1. However, it is conceivable that a condensed equivalent extends out onto the oceanic crust in the Guyana–Suriname Basin. Defining the exact age of the Jurassic oceanic crust in the Guyana–Suriname Basin is problematic due to the lack of basement penetrations and magnetic anomalies. Based on the east–west spreading axis of the Central Atlantic, it can be assumed that oceanic crust becomes younger into the basin towards the NW.

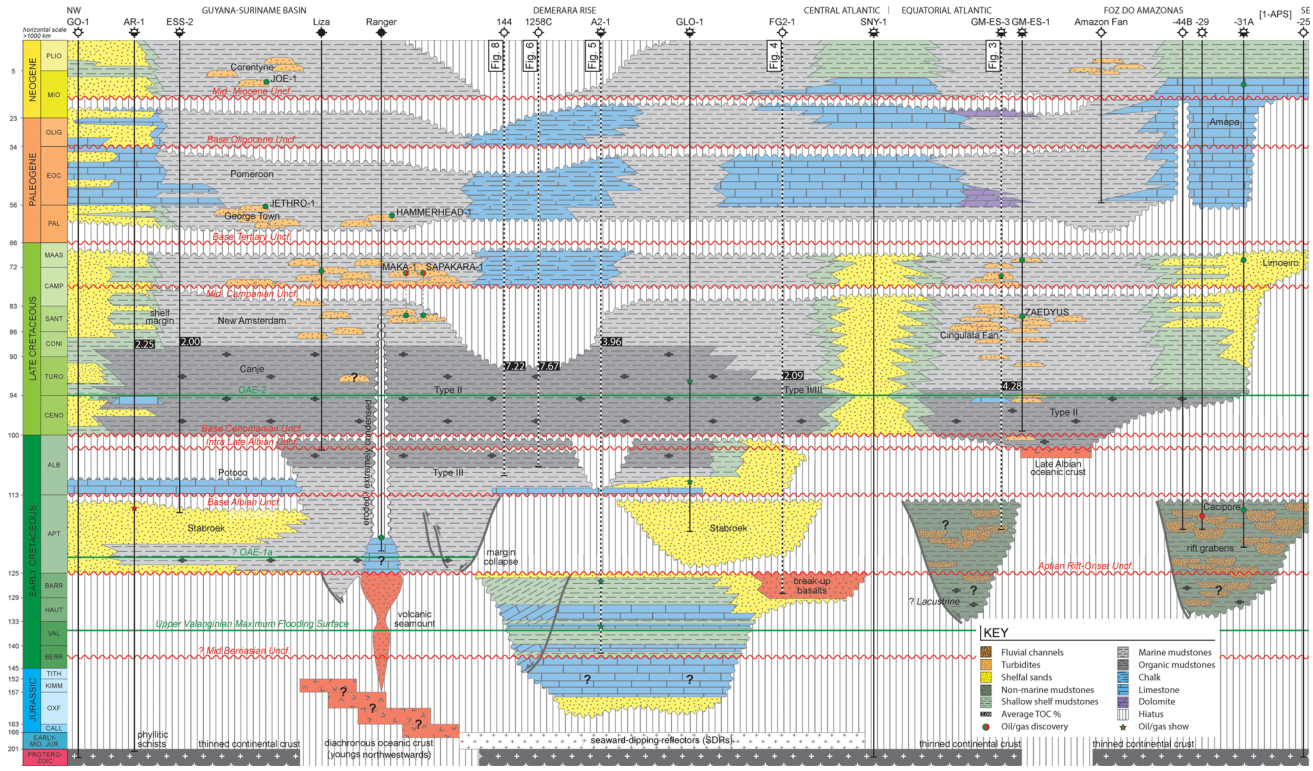

Fig. 15. A Wheeler diagram constructed along strike from Guyana (left) to Brazil (right) detailing the stratigraphic evolution of the segmented Guyanas continental margin. The pin-stripe vertical lines indicate hiatus' corresponding to various regional unconformities dated in the stratigraphic analysis. The dashed black and white lines indicate revised wells in this study. The geological timescale (GTS 2018) is non-linear. Hydrocarbon occurrences are shown. Average TOC values for the Canje Formation are displayed; AR-1 data are from Mourlot (2018).

Further heterogeneity along strike is apparent at the Aptian unconformity. In the Equatorial Atlantic domain, as penetrated by the 1-APS wells, the first deposits within the synrift half-graben are non-marine mudstones, with postulated lacustrine-sourced organic material encountered further along the Equatorial margin (Pasley *et al.* 2004; Dickson *et al.* 2016), followed by coarser siliciclastics deposited in fluvial channel and alluvial fan systems of the Cacipore Formation. Contiguous, time-equivalent deposits in the Central Atlantic domain belong to the Stabroek Formation, a unit of progradational fluvio-deltaic sands. We assume an Aptian age for the oil-bearing carbonate reservoir encountered in Ranger-1, which built-up above a volcanic seamount in the deep basin. Early Albian Potoco Formation shallow-marine limestones, as described from A2-1, are the transgressive deposits that were deposited above the regional BAU. These deposits are restricted to the shallow-water areas of the Demerara Rise and Guyana Shelf. Time-equivalent shelfal sands are located more proximally (GLO-1 and FG2-1: Fig. 15).

The onset of organic-rich sedimentation is well calibrated at ODP Site 1258C to commence during the late Middle Albian (Fig. 6). Deep-water Late Albian deposition was established in the adjacent French Guiana Basin associated with localized turbidites. Marine flooding of this basin and creation of oceanic crust outboard of the GM-ES wells is coincident with the intra-Late Albian Unconformity recognized across the Demerara Rise (Figs 6 and 7). The BCU truncates the Late Albian stratigraphy along the Guyana Shelf and Demerara Rise, coeval with the final continental break-up (unlocking) of the African and South American plates (Geognostics 2020) at the Demerara Rise–Guinea Plateau. At this time, a short-lived compressional phrase is recognized along the Romanche Fracture Zone within the Equatorial Atlantic (Davison *et al.* 2016). By earliest Cenomanian times oceanic crust is contiguous between the Central Atlantic and Equatorial Atlantic. Organic-rich sedimentation persists into the Coniacian within the Guyana–Suriname Basin and onto the Demerara Rise, forming the prolific source rock of the Canje Formation, and continues even younger into the Upper Santonian further NW in Venezuela (La Luna facies). Cessation of organic-rich sedimentation is diachronous along the margin: organic levels in FG2-1 decrease during the late Turonian, and even earlier in the early Turonian within the Equatorial Atlantic domain. Subsequent establishment of deep-water turbidite depositional systems (i.e. submarine channel–lobe–fan systems) characterize the Late Cretaceous succession, hosting significant oil discoveries within the New Amsterdam Formation.

Deep-water sands overlie the MCU, related to a significant hiatus observed across the Demerara Rise. Although not re-evaluated in this study, several significant unconformities through the Cenozoic are regionally distinguished, often linked to sandstone reservoir development within the overlying sequence (i.e. George Town and Corentyne formations). Throughout the Cenozoic, shelfal carbonates replace previously siliciclastic-dominated systems, and shallow-marine chalks are present over the Demerara Rise.

Palaeogeographical reconstructions

A series of gross depositional environment (GDE) maps (Fig. 16) have been constructed at four key time intervals during the Cretaceous recognized in the stratigraphic analysis (Fig. 2). These events are either major sequence boundaries or MFSs, representing the environment of deposition during maximum regression or transgression, respectively. Four types of environment are described in this study: terrestrial, transitional, slope and deep basin with their sand fairways (submarine canyon, channel to fan systems). These environmental interpretations are primarily based on the well data and seismic evidence presented in this study, as well as on the incorporation of additional published data. Facies distributions (pies) for wells that penetrate sediments of each age interval are added as control points; however, there may be additional

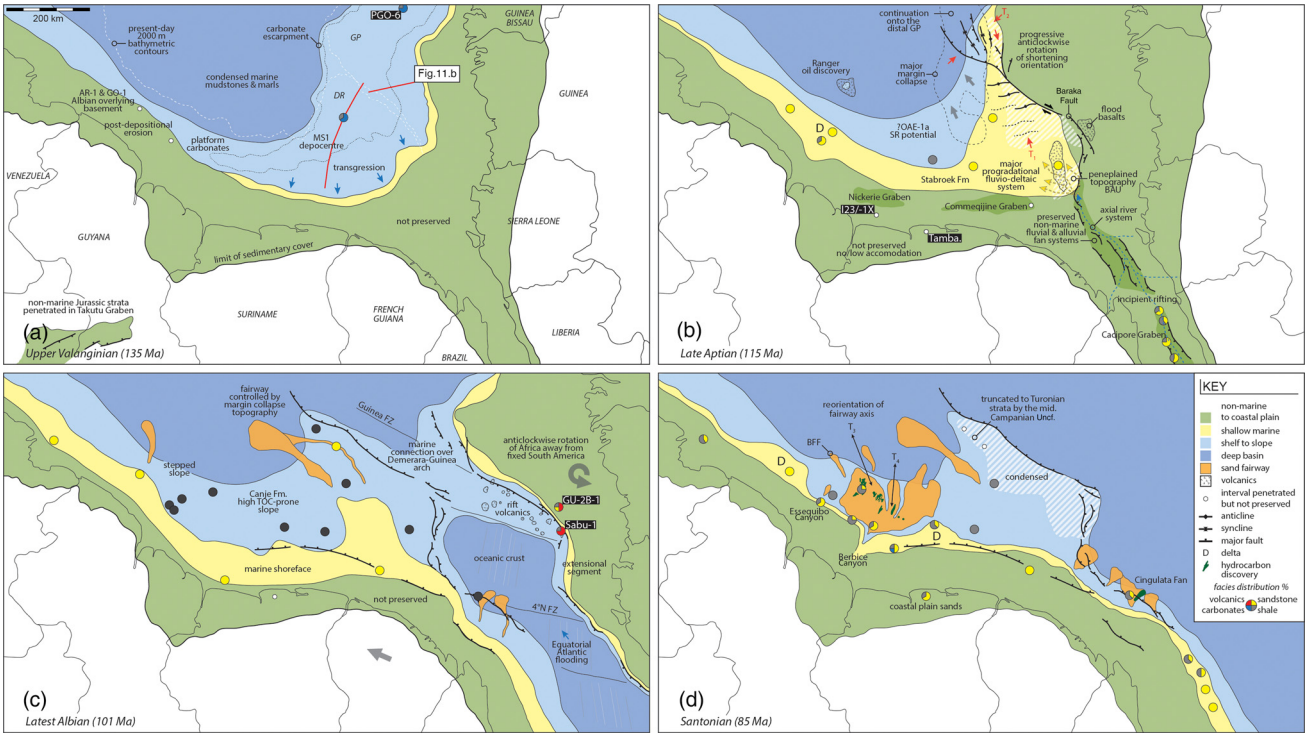

Fig. 16. Gross depositional environment (GDE) maps for four key time stages, defined by the stratigraphic analysis, in the evolution of the Guyanas continental margin: (**a**) upper Valanginian (135 Ma), (**b**) Aptian (115 Ma), (**c**) latest Albian (101 Ma) and (**d**) Santonian (85 Ma). The reconstructed locations of the conjugate seismic sections (Fig. 11b) are displayed in (a). The facies distribution (%) for the interval encountered in each well is shown. Geometries were reconstructed following the Geognostics Earth Model (GEM™). BFF, basin-floor fan; DR, Demerara Rise; FZ, fracture zone; GP, Guinea Plateau.

penetrations of the stratigraphy unavailable in this study. As the individual depositional systems have been described earlier, a more holistic review of the regional geology is discussed below.

Upper Valanginian

The conjugate Demerara Rise and Guinea Plateau formed a carbonate-dominated shallow-marine embayment extending *c.* 300 km from the palaeocoastline to the shelf margin. The maximum extent of the southeastern proto-Central Atlantic Ocean prior to Equatorial Atlantic opening and breakthrough is defined by the coastline shown in Figure 16a. Due to the gravitational margin collapse, an interpretation of the carbonate shelf margin architecture is restricted; however, a carbonate escarpment geometry is documented to the north in The Gambia and to the west in Guyana (Mourlot 2018; Mourlot *et al.* 2018; Casson *et al.* 2020*a*). The extension of the major depocentre below the majority of the Guinea Plateau (Fig. 16a) (Zinecker and Mann 2020) indicates continuous and synchronous deposition linking the conjugate margins, challenging the interpretation by Gouyet *et al.* (1994) that a local high was present between the Demerara Rise and Guinea Plateau. Lower Cretaceous strata are absent due to post-depositional erosion across the Guyana Shelf.

Late Aptian

Rift initiation to the east in the Equatorial Atlantic created an oblique-slip stress regime that exerted transpression-related compression along the Demerara–Guinea transform, leading to the northwestward gravitational collapse of the Demerara Rise margin. A similar gravitational margin collapse feature is recognized from seismic data on the Guinea Plateau (Zinecker and Mann 2020; Casson 2020*b*). The topography generated by this feature on the Guinea Plateau remains reflected in the present-day bathymetry, forming an 'outer high' (Long *et al.* 2018). Progressive anticlockwise rotation of Africa away from South America continued to deform the transform margins of the Demerara Rise and Guinea Plateau (Pindell 1985; Greenroyd *et al.* 2007, 2008; Basile *et al.* 2013). Equatorial Atlantic rifting is likely to have rejuvenated sediment supply from the Guiana Shield, resulting in progradation of the fluvio-deltaic systems of the Stabroek Formation (MS2) into the Guyana–Suriname Basin. This system was likely to have been fed by a major axial fluvial system interpreted as running through the Cacipore Graben northwestwards into French Guiana, with associated non-marine and fluvial sediments preserved within the rifting-induced accommodation. Coastal plain strata are not preserved due to no or low accommodation as recorded in wells I23/-1X, SNY-1 and Tambaredjo (Dronkert and Wong 1993). Associated exhumation of the hinterland is supported by low-temperature thermochronological data from the northern rim of the Guiana Shield in French Guiana, where Derycke *et al.* (2018) recorded a major cooling event which suggesting that exhumation occurred from 140 to 100 Ma.

Latest Albian

During this time, elevated organic levels were established in sediments deposited across the shelf to slope environment, evidenced in the studied scientific boreholes. A stepped slope was established along the Guyana–Suriname margin. Deposition of a major submarine channel–fan system was controlled by the antecedent topography generated by the collapsed margin. Rift volcanics observed on seismic are also interpreted throughout the opening Demerara–Guinea oceanic domain segment (Olyphant *et al.* 2017) (Fig. 16c). Adjacent continental margins are narrow and fault controlled within the extensional basin.

At this time, models of magnetic anomalies in the oceanic crust (Müller *et al.* 2008) predict that seafloor spreading initiated in the extensional segment offshore French Guiana between 110 and

105 Ma (Albian). The relatively thick (*c.* 200 m) latest Albian (early NC10a) deep-marine section documented in GM-ES-3 (Fig. 11a) unconformably, based on seismic interpretation, overlies undated non-marine synrift strata. The well is located above thinned continental crust (Fig. 11a). This interval (NC10a) is highly condensed, only 0.55 m thick, on the Demerara Rise above an intra-Late Albian unconformity (Fig. 7). We suggest that the creation of accommodation offshore French Guiana and subsequent filling with latest Albian deep-marine deposits indicates an early Late Albian age (i.e. pre-intra-Late Albian Unconformity) for the onset of seafloor spreading and oceanic crust formation. It remains to be understood whether the late Albian marine connection between the Central and Equatorial Atlantic occurred over a flooded Demerara Rise or through an open Demerara–Guinea transform. The conjugated Demerara Rise and Guinea Plateau was likely to have been the final buttress preventing the establishment of a deep-water connection between the Equatorial and Central Atlantic, this deep-water connection was only established with the final phase of oceanic crust formation at the beginning of the Cenomanian; this event is represented by the BCU across the Demerara Rise (Fig. 15).

Santonian

By Santonian times (Fig. 16d) Africa has drifted away from South America, forming a deep-water connection between the North and South Atlantic oceans. The Late Cretaceous sequence is highly condensed and the MCU is observed in wells across the distal Demerara Rise due to it remaining as a palaeohigh. This period is associated with deposition of extensive submarine fan–channel systems in the basin. These systems offshore French Guiana are relatively narrow and steep in comparison to their Suriname–Guyana counterparts, perhaps corresponding to the length and volume of the onshore drainage system (Sømme *et al.* 2009). Entry points for these systems breach relay zones between rift faults along the Equatorial Atlantic margin. The channels of these short systems erode and remove the underlying organic-rich interval, as observed in GM-ES-3 (Fig. 3). The deep-water systems in Suriname–Guyana form the prolific hydrocarbon reservoirs encountered in the Stabroek Block. Updip, these systems are fed through the Berbice and Essequibo canyons, depositing sand in submarine channel complexes across the slope to basin-floor fans. A reorientation and retrogression of this fairway axis is observed through the Late Cretaceous, postulated to be related to a decrease in sediment supply through the Berbice Canyon and compensational stacking (T_3, Albian–Turonian; T_4, Coniacian–Maastrichtian: Mourlot 2018).

Discussion

Comparison of the conjugate margin–Guinea Plateau

Although seismic reflection or well data from the Guinea Plateau were not available for this study, a review of material previously published allows both of the conjugate margins to be examined in light of our new findings. Analysis of seismic lines (Fig. 11) on the Demerara Rise, SR1-5400 (GuyanaSPAN), and lines from the Guinea Plateau presented in Edge (2014), reconstructed to their position at pre-Equatorial Atlantic rifting times (i.e. pre-Aptian), reveals that these lines align as 'conjugates' (Fig. 16a). This has been used to supplement the GDE mapping of the Guinea Plateau (Fig. 16). Although seismic imaging quality of the deep basement structure below the Guinea Plateau is poor, preventing detailed analysis, exploration wells on the southern margin of the Guinea Plateau (GU-2B-1, Sabu-1 and Fatala-1: Fig. 16c) targeted the post-rift sequence. Calibration of the oldest strata is extrapolated from wells PGO-2 and PGO-6, reaching TD in Jurassic micritic limestones and shale (Zinecker and Mann 2020). Notably, both Long *et al.* (2018) and Zinecker and Mann (2020), during their regional seismic interpretation of 2D seismic data across the Guinea Plateau, identified NW-dipping SDR sequences underlying the Jurassic carbonate sequence (approximating to MS1), consistent with the dip orientation of the basement sequence below the Demerara Rise (Reuber *et al.* 2016). Several major SW-dipping listric faults (i.e. Baraka Fault: Fig. 16b) are observed on the southern rifted margin of the Guinea Plateau; Olyphant *et al.* (2017) interpreted these thick-skinned, subvertical faults to penetrate into oceanic basement. These faults within the transform truncate thick crust (i.e. not gradually thinned continental crust as observed on rifted margins). The geometry of the Demerara–Guinea transform faults and narrow conjugate continental margins appear similar; however, the first major faults that develop at the continental–oceanic transition have reverse polarities: that is, the faults near the Guinea Plateau continent–ocean boundary dip landwards (Zinecker and Mann 2020), whereas on the Demerara Rise they dip towards the oceanic basin, highlighting the margin asymmetry (Fig. 11b).

Our interpretation is that the mapped Top Neocomian horizon of Edge (2014) represents the Valanginian flooding surface, based on the correlation of seismic facies and architecture (Fig. 11b). Below the BAU, the Aptian unconformity and overlying synrift wedge is penetrated in well GU-2B-1 on the Guinea Plateau (Fig. 11b). These synrift strata are only preserved basinward of the east–west-trending Baraka Fault (see fig. 3 in Olyphant *et al.* 2017), are likely to be analogous to the synrift strata offshore French Guiana (Fig. 11a) and correlate with the pre-Albian Cacipore Formation in the Foz do Amazonas Basin (Fig. 15). Within this sequence, break-up-related basalts and volcaniclastics are penetrated in wells GU-2B-1 and Sabu-1 (Olyphant *et al.* 2017), distributed along the southern margin of the Guinea Plateau (Fig. 16c) (Benkhelil *et al.* 1995; Gouyet *et al.* 1994). The apparent lack of any Aptian compressional deformation on the conjugate margin seismic profile (Fig. 11b) is probably due to its position, as the majority of the deformation is located on the SW nose of the Guinea Plateau (Fig. 16b) (cf. Zinecker and Mann 2020). There is a considerable difference in the Cenozoic sediment thickness (Fig. 11b); pro-gradational sigmoidal seismic reflections (clinoforms) on the Demerara Rise indicate the deposition of a major shelfal siliciclastic system penetrated in well GLO-1, leading to the deeper burial of pre-Cenozoic stratigraphy.

Margin heterogeneity influenced by structural inheritance

Evaluating the margin architecture at a super-regional scale (i.e. >1000 km along strike) highlights the heterogeneities that result in the segmentation of continental margins (e.g. Watts and Stewart 1998; Franke *et al.* 2007; Faleide *et al.* 2008). From this study, spatial variabilities are recorded in the depositional systems (Fig. 16), associated drainage systems onshore, structural style (Figs 13 and 14) and organic matter distribution (Fig. 9). Further studies show that segmentation causes additional variations in subsidence history (Tsikalas *et al.* 2001; Pereira and Alves 2011). Sedimentation over the Demerara Rise, particularly the more distal section, is heavily condensed with low sedimentation rates (Fig. 2), and many Cretaceous–recent post-rift unconformities are recorded (Fig. 11). These redated surfaces are interpreted to be sequence boundaries developed at lowstands that can be correlated with increased siliciclastic delivery into the adjacent deep-water basins (Vail *et al.* 1980). Additionally, the margins of the Demerara Rise were the focus of repeated tectonic deformation, developing both transpressional and extensional fault systems, during Equatorial Atlantic break-up (Fig. 16). Internal deformation of the Demerara Rise is diverse, ranging from broad long-wavelength folding to tight imbricate thrust fault systems (Fig. 13). Fundamentally, the stratigraphic and structural heterogeneities discussed are

consequential of the pre-rift structural inheritance, eventually modified by the dual-phase rifting history.

The Demerara Rise and its conjugate, the Guinea Plateau, are thought to have formed a focal point for hotspot magmatism (CAMP or Bahamas hotspot related) during the early stages of the Central Atlantic opening, potentially creating a volcanic accumulation up to 21 km thick (Reuber *et al.* 2016; Long *et al.* 2018; Zinecker and Mann 2020). These submarine plateaus are clearly identifiable in present-day bathymetric maps, being a testament to the longstanding influence this basement configuration had on the bathymetry and, ultimately, the segmentation of the continental margin, as observed on other TMPs worldwide (Loncke *et al.* 2020). The location of the volcanism in the southeastern Central Atlantic has been interpreted as creating a 'pinning point' for the final fragmentation of Gondwana and the break-up of the Equatorial Atlantic segment (Pindell 1985; Greenroyd *et al.* 2007, 2008; Basile *et al.* 2013). It is conceivable that the Jurassic volcanism created a crustal weakness exploited during the second Equatorial phase of rifting. Similar segmentation of continental margins and its effects on post-rift deposition are documented globally from the rifted Norwegian (Tsikalas *et al.* 2001), western India (Calvès *et al.* 2011), Levant (Ben-Avraham *et al.* 2006) and Uruguayan margins (Soto *et al.* 2011).

Conclusions

New stratigraphic analysis by resampling seven exploration wells and scientific boreholes located along the Guyanas continental margin of South America has been used to refine a high-resolution Jurassic–Cretaceous stratigraphic framework, applicable to the Central Atlantic. This framework is applied to the interpretation of a margin-scale 2D deep seismic reflection survey to produce a new megasequence architectural model, create updated palaeogeographical reconstructions for four key geological intervals and reconstruct the structural evolution through the two divergent phases of break-up during the Jurassic (Central Atlantic) and Cretaceous (Equatorial Atlantic).

Our findings highlight that deposition during the early Central Atlantic post-rift sequence (Jurassic–Lower Cretaceous, i.e. MS1) was influenced by the underlying heterogeneous basement structure, composed of thinned continental crust and volcanic addition in the form of thick SDR sequences. The major MS1 depocentre below the Demerara Rise that continues below the conjugate Guinea Plateau passively infilled pre-existing basement topography. The only well on the South American margin to penetrate this sequence is the A2-1 well. New multiproxy biostratigraphy data conclusively reveals that the well reached total depth in late Tithonian organic-lean (average TOC 0.37%) shales and limestones. Previous work that suggested A2-1 penetrated a Jurassic-aged source rock is questioned by this new integrated dataset. MS1 is capped by a super-regional MFS during the upper Valanginian (VF), recognized elsewhere around the Central Atlantic and Gulf of Mexico. The landward limit of the MFS reveals the southeastern extension of the early Central Atlantic.

Rifting in the Equatorial Atlantic during Barremian–Aptian times modified the continental margin architecture, the structure and succeeding depositional systems. Deep pre-Albian graben formed along the proto-Equatorial margins, receiving continental sedimentation. Further associated break-up volcanism is evidenced by 125 Ma basalts recovered in the French Guiana FG2-1 well. The progressive anticlockwise rotation of Africa from South America during the Aptian induced a transpressional regime causing an estimated 8.3 km of shortening across the distal Demerara Rise. This tectonism resulted in short-wavelength folding and thrusting, major gravitational margin collapse into adjacent basins, and the formation of a progradational shelfal siliciclastic system (Stabroek Formation). This sequence (MS2) is truncated by a super-regional angular unconformity re-dated as basal Albian (BAU), peneplaning up to 1 km of sediment from the Demerara Rise.

At GM-ES-3, the rapid facies change from rifted continental deposits into Late Albian deep-water deposits is a possible reflection of the creation of oceanic crust outboard in the extensional segment of the opening Equatorial Atlantic offshore French Guiana and associated rapid subsidence of the basin margin. This event is represented by the time-synchronous intra-Late Albian Unconformity recognized on the Demerara Rise. Our model suggests that final break-up of the Demerara Rise and Guinea Plateau, and deep marine connection between the Equatorial and Central Atlantic, occurred during the earliest Cenomanian following unlocking of the Demerara–Guinea transform.

The distal Demerara Rise sedimentary sequence is highly condensed and contains multiple unconformities dated as middle Campanian (MCU), base Tertiary (BTU) and middle Miocene (MMU), suggesting that this area remained an area of low accommodation and a relative high, probably due to the anonymously thick crust. Onset of organic-rich sedimentation (Canje Formation) co-occurred with the flooding of the Equatorial Atlantic (pre-oceanic crust formation) during the late Middle Albian. Geochemical characterization of these primarily marine Type II organic-rich strata (average TOC 4.21%) shows heterogeneity along strike, reflecting sediment dilution and terrestrial organic matter input.

The topography generated by the gravitational margin collapse is interpreted to have been a major control on the entry point of siliciclastic delivery, funnelling sediment from the shallow Demerara Rise into the deep-water sedimentary systems of the Guyana–Suriname Basin. The Berbice Canyon has already been described from previous studies as another major sediment input point throughout the Late Cretaceous, delivering sediment to the world-class hydrocarbon reservoirs in the Guyana–Suriname Basin. Coeval siliciclastic input occurred along the Equatorial margin, and the depositional systems display relatively short runout lengths, related to the steep, narrow margin geometry.

Examining the sedimentary systems using this integrated approach at a margin-scale reveals the important control of inherited pre-rift structural and basement heterogeneity, and later structural evolution associated with the second phase of break-up, on the post-rift depositional system distribution and overall margin heterogeneity.

Acknowledgements This study is part of M. Casson's PhD project at the University of Manchester. The companies of the North Africa Research Group (NARG) are thanked for their continued scientific support. Holger Kuhlmann provided excellent support during our visits to the Bremen Core Repository and subsequent requests for additional samples. Shell is thanked for the access to hydrocarbon exploration well data, particularly Tyrone Sigur at the CGG storage facility, Schulenburg, Texas. Iain Prince and Peter Osterloff (Shell) are thanked for their attentive support, and, in addition, David Owen and Robert Campbell (Shell) helped to improve our manuscript. The seismic data presented is courtesy of ION Geophysical. Ian Mounteney is acknowledged for his assistance in performing the XRD analysis at the British Geological Survey, Keyworth, UK. Alastair Bewsher at the University of Manchester is thanked for use of the organic geochemistry laboratory. Discussion with Jon Teasdale and academic access to the Geognostics Earth Model (GEM™) were particularly useful in understanding the regional geology, plate tectonics and structure. Frédéric de Ville de Goyet thanks Nick Miles, Petrostrat, for assistance in the Lower Cretaceous palynology. Professor David Wray, Greenwich University, is acknowledged for his assistance in running the pyrolysis. Jim Armstrong is acknowledged for his assistance interpreting the organic geochemistry results. Aruna Mannie (Premier Oil) and Paul Mann (University of Houston) are thanked for their constructive reviews that improved the clarity of this paper.

Author contributions **MC**: conceptualization (lead), data curation (lead), formal analysis (lead), investigation (lead), methodology (lead), project administration (lead), resources (lead), writing – original draft (lead); **JJ**: conceptualization (supporting), formal analysis (equal), investigation (supporting), supervision (supporting), writing – original draft (supporting); **GC**: conceptualization (supporting), supervision (equal), writing – review &

editing (supporting); **FDVDG**: formal analysis (supporting), writing – original draft (supporting); **KR**: data curation (supporting), formal analysis (supporting), supervision (supporting); **MB**: formal analysis (supporting), writing – original draft (supporting); **DR**: formal analysis (supporting), writing – original draft (supporting); **LB**: supervision (supporting), writing – review & editing (supporting); **JR**: funding acquisition (supporting), supervision (supporting), writing – review & editing (supporting).

Funding The sponsoring companies of the North Africa Research Group (NARG) are thanked for their continued financial support. The sampling and subsequent analysis of DSDP/ODP cores was partially supported by a European Consortium for Ocean Research Drilling (ECORD) research grant awarded to M. Casson. D. Reháková was supported by the VEGA 2/2013/20 Project. Cairn Energy are thanked for funding the hydrocarbon extractions at GeoMark Research.

Data availability The data that support the findings of this study are available from ION Geophysical but restrictions apply to the availability of these data, which were used under licence for the current study and so are not publicly available. Data are, however, available from the authors upon reasonable request and with permission of ION Geophysical.

References

Allen, P.A. and Allen, J.R. 2013. *Basin Analysis: Principles and Application to Petroleum Play Assessment*. John Wiley & Sons, Chichester, UK.

Ando, A., Huber, B.T., MacLeod, K.G. and Watkins, D.K. 2015. Early Cenomanian 'hot greenhouse' revealed by oxygen isotope record of exceptionally well-preserved foraminifera from Tanzania. *Paleoceanography*, **30**, 1556–1572, https://doi.org/10.1002/2015PA002854

Armstrong H. and Brasier, M. 2013. *Microfossils*. John Wiley, New York.

Bally, A.W. 1981. Atlantic-type margins. *AAPG Special Volumes*, **123**, 1–48.

Basile, C., Mascle, J. and Guiraud, R. 2005. Phanerozoic geological evolution of the Equatorial Atlantic domain. *Journal of African Earth Sciences*, **43**, 275–282, https://doi.org/10.1016/j.jafrearsci.2005.07.011

Basile, C., Maillard, A. *et al.* 2013. Structure and evolution of the Demerara Plateau, offshore French Guiana: Rifting, tectonic inversion and post-rift tilting at transform–divergent margins intersection. *Tectonophysics*, **591**, 16–29, https://doi.org/10.1016/j.tecto.2012.01.010

Basile, C., Girault, I., Paquette, J.L., Agranier, A., Loncke, L., Heuret, A. and Poetisi, E. 2020. The Jurassic magmatism of the Demerara Plateau (offshore French Guiana) as a remnant of the Sierra Leone hotspot during the Atlantic rifting. *Scientific Reports*, **10**, 1–12, https://doi.org/10.1038/s41598-020-64333-5

Behar, F., Beaumont, V. and Penteado, H.D.B. 2001. Rock-Eval 6 technology: performances and developments. *Oil & Gas Science and Technology*, **56**, 111–134, https://doi.org/10.2516/ogst:2001013

Below, R. 1982: Scolochorate Zysten der Gonyaulacaceae (Dinophyceae) aus der Unterkreide Marokkos. *Palaeontographica Abteilung B*, **182**, 1–51, pl. 1–9.

Ben-Avraham, Z., Schattner, U., Lazar, M., Hall, J.K., Ben-Gai, Y., Neev, D. and Reshef, M. 2006. Segmentation of the Levant continental margin, eastern Mediterranean. *Tectonics*, **25**, TC5002, https://doi.org/10.1029/2005TC001824

Benkhelil, J., Mascle, J. and Tricart, P. 1995. The Guinea continental margin: an example of a structurally complex transform margin. *Tectonophysics*, **248**, 117–137, https://doi.org/10.1016/0040-1951(94)00246-6

Bihariesingh, V. 2014 Is the Cretaceous an Effective Petroleum System Offshore Suriname? *AAPG Datapages/Search and Discovery*, 30355

Bland, S., Griffiths, P. and Hodge, D. 2004. Restoring the seismic image with a geological rule base. *First Break*, **22**, https://doi.org/10.3997/1365-2397.22.4.25845

Blau, J. and Grün, B. 1997. Neue Involutinen (Foraminifera) aus dem marmorea-Hartgrund (Hettangium/Sinemurium, Lias) von Adnet (Österreich). *Neues Jahrbuch für Geologie und Paläontologie-Abhandlungen*, **45**, 247–262, https://doi.org/10.1127/njgpa/204/1997/247

Bown, P. 1998. *Calcareous Nannofossil Biostratigraphy*. Kluwer Academic, Dordrecht, The Netherlands.

Bown, P.R. 2001. Calcareous nannofossils of the Gault, Upper Greensand and Glauconitic Marl (Middle Albian–Lower Cenomanian) from the BGS Selborne boreholes, Hampshire. *Proceedings of the Geologists' Association*, **112**, 223–236, https://doi.org/10.1016/S0016-7878(01)80003-1

Bralower, T.J., Sliter, W.V., Arthur, M.A., Leckie, M.R., Allard, D. and Schlanger, S.O. 1993. Dysoxic/anoxic episodes in the Aptian–Albian (Early Cretaceous). The Mesozoic Pacific. Geology, tectonics and volcanism. *American Geophysical Union Geophysical Monograph Series*, **77**, 5–37.

Burk, K. and Dewey, J.F. 1974. Two plates in Africa during the Cretaceous? *Nature*, **249**, 313–316, https://doi.org/10.1038/249313a0

Burnett, J.A., 1998. Upper Cretaceous. *In*: Bown, P.R. (ed.) *Calcareous Nannofossil Biostratigraphy*. Kluwer Academic, Dordrecht, The Netherlands, 132–199.

Calvès, G., Schwab, A.M. *et al.* 2011. Seismic volcanostratigraphy of the western Indian rifted margin: The pre-Deccan igneous province. *Journal of Geophysical Research: Solid Earth*, **116**, B01101, https://doi.org/10.1029/2010JB000862

Casson, M., Calvès, G., Huuse, M., Sayers, B and Redfern, J. 2020*a*. Cretaceous continental margin evolution revealed using quantitative seismic geomorphology, offshore northwest Africa. *Basin Research*, **33**,66–90,https://doi.org/10.1111/bre.12455

Casson, M.A. 2020*b*. *Tectono-stratigraphic evolution of the Mesozoic continental margins of the Central Atlantic*. PhD thesis, University of Manchester.

Cedeño, A.F., Ohm, S.E., Escalona, A. and Narain, E. 2019. Petroleum system (s?) in the Guyana–Suriname Basin: Insights from a geochemical study onshore Suriname. *In*: Proceedings of the 29th European Association of Geoscientists and Engineers International Meeting on Organic Geochemistry, September 2019. EAGE, Houten, The Netherlands, https://doi.org/10.3997/2214-4609.201902838

CGMW–CPRM–DNPM 2003. *1:5 500 000 Geological Map of South America*. Commission for the Geological Map of the World (CGMW). Geological Survey of Brazil (CPRM), National Department of Mineral Production, Brazil (DNPM)

Charton, R.J.G. 2018. *Phanerozoic Vertical Movements in Morocco*. Doctoral thesis, TU Delft, Delft, The Netherlands.

Chin, S., 2016. *Upper Albian to Lower Cenomanian Calcareous Nannofossil Biostratigraphy of the Proto-North Atlantic*. MSc thesis, The University of Nebraska-Lincoln.

Clemson, J., Cartwright, J. and Booth, J. 1997. Structural segmentation and the influence of basement structure on the Namibian passive margin. *Journal of the Geological Society, London*, **154**, 477–482, https://doi.org/10.1144/gsjgs.154.3.0477

Cordani, U.G., Ramos, V.A. *et al.* 2016. *Tectonic Map of South America*. Commission for the Geological Map of the World.

Costa, L. I. and Davey, R. J., 1992. Dinoflagellate cysts of the Cretaceous System. *In*: McIntyrepowel, A. J. (eds) *A Stratigraphic Index of Dinoflagellate Cysts*. Chapman and Hall, London, 99–131.

Davey, R.J. 1982. Dinocyst stratigraphy of the latest Jurassic to Early Cretaceous of the Haldager No. 1 borehole, Denmark. *Danmarks Geologiske Undersøgelse, Series B*, **6**, 1–57, pl. 1–10.

Davison, I. 2005. Central Atlantic margin basins of North West Africa: geology and hydrocarbon potential (Morocco to Guinea). *Journal of African Earth Sciences*, **43**, 254–274, https://doi.org/10.1016/j.jafrearsci.2005.07.018

Davison, I., Faull, T., Greenhalgh, J., Beirne, E.O. and Steel, I. 2016. Transpressional structures and hydrocarbon potential along the Romanche Fracture Zone: a review. *Geological Society, London, Special Publications*, **431**, 235–248, https://doi.org/10.1144/SP431.2

Derycke, A., Gautheron, C.., Bourbon, P., Pinna-Jamme, R., Aertgeerts G. and Simon-Labric, T. 2018. French Guyana margin evolution: insight by low-temperature thermochronological data. Presented at Thermo 2018: 16th International Conference on Thermochronology, 16–21 September 2018, Quedlinburg, Germany.

Dickson, W., Schiefelbein, C.F., Odegard, M.E. and Zumberge, J.E. 2016. Petroleum systems asymmetry across the South Atlantic Equatorial Margins. *Geological Society, London, Special Publications*, **431**, 219–233, https://doi.org/10.1144/SP431.13

Dodekova, L. 1969. Dinoflagellés et acritarches du Tithonique aux environs de Pleven, Bulgarie central du nord. Bulgarska Akademiya na Naukite, Izvestiya na Geologicheskiya Institut, *Seriya Paleontologiya*, **18**, 13–24, pl. 1–5.

Doyle, J. A., Jardiné, S. and Doerenkamp, A. 1982. Afropollis, a new genus of early angiosperm pollen, with notes on the Cretaceous palynostratigraphy and paleoenvironments of Northern Gondwana. *Bulletin des Centres Recherches Exploration–Production Elf Aquitaine*, **6**, 39–117.

Dronkert, H. and Wong, T.E. 1993. Geology of the Tambaredjo oil field, Suriname. *AAPG Bulletin*, **77**.

Duxbury, S. 1983. A study of dinoflagellate cysts and acritarchs from the Lower Greensand (Aptian to Lower Albian) of the Isle of Wight, southern England. *Palaeontographica Abt. B*, **186**, 18–80.

Edge, R. 2014. *Rifting of the Guinea Margin in the Equatorial Atlantic from 112 to 84 Ma: Implications of Paleo-Reconstructions for Structure and Sea-Surface Circulation*. PhD thesis, University of Arizona, Tucson, Arizona, USA, retrieved from http://hdl.handle.net/10150/321395

Erbacher, J., Mosher, D.C. *et al.*. 2004*a*. Demerara Rise; equatorial Cretaceous and Paleogene paleoceanographic transect, western Atlantic; covering Leg 207 of the cruises of the drilling vessel JOIDES Resolution; Bridgetown, Barbados, to Rio de Janeiro, Brazil; Sites 1257–1261; 11 January–6 March 2003. *In*: Chapman, M. and Peters, L. L. (eds) *Proceedings of the Ocean Drilling Program (ODP) Initial Reports, Part A-207*. Ocean Drilling Program, College Station, TX, 1–89.

Erbacher, J., Mosher, D.C. *et al.*. 2004*b*. Site 1258. *In*: Chapman, M. and Peters, L. L. (eds) *Proceedings of the Ocean Drilling Program (ODP) Initial Reports, Part A-207*. Ocean Drilling Program, College Station, TX, 1–117.

Erbacher, J., Friedrich, O., Wilson, P.A., Birch, H. and Mutterlose, J. 2005. Stable organic carbon isotope stratigraphy across Oceanic Anoxic Event 2 of Demerara Rise, western tropical Atlantic. *Geochemistry, Geophysics, Geosystems*, **6**, Q06010, https://doi.org/10.1029/2004GC000850

Erlich, R. N., Villamil, T. and Keens-Dumas, J. 2003. Controls on the deposition of Upper Cretaceous organic carbon-rich rocks from Costa Rica to Suriname. *AAPG Memoirs*, **79**, 1–45.

Esso 1978. Demerara A2-1 well report.

Faleide, J.I., Tsikalas, F. *et al.* 2008. Structure and evolution of the continental margin off Norway and the Barents Sea. *Episodes*, **31**, 82–91, https://doi.org/10.18814/epiiugs/2008/v31i1/012

Fanget, A.S., Loncke, L. *et al.* 2020. A synthesis of the sedimentary evolution of the Demerara Plateau (Central Atlantic Ocean) from the Late Albian to the Holocene. *Marine and Petroleum Geology*, **114**, 104–195, https://doi.org/10.1016/j.marpetgeo.2019.104195

Figueiredo, J.J.J.P., Hoorn, C., Van der Ven, P. and Soares, E. 2009. Late Miocene onset of the Amazon River and the Amazon deep-sea fan: Evidence from the Foz do Amazonas Basin. *Geology*, **37**, 619–622, https://doi.org/10.1130/G25567A.1

Franke, D. 2013. Rifting, lithosphere breakup and volcanism: Comparison of magma-poor and volcanic rifted margins. *Marine and Petroleum Geology*, **43**, 63–87, https://doi.org/10.1016/j.marpetgeo.2012.11.003

Franke, D., Neben, S., Ladage, S., Schreckenberger, B. and Hinz, K. 2007. Margin segmentation and volcano-tectonic architecture along the volcanic margin off Argentina/Uruguay, South Atlantic. *Marine Geology*, **244**, 46–67, https://doi.org/10.1016/j.margeo.2007.06.009

Friedrich, O. and Erbacher, J. 2006. Benthic foraminiferal assemblages from Demerara Rise (ODP Leg 207, western tropical Atlantic): possible evidence for a progressive opening of the Equatorial Atlantic Gateway. *Cretaceous Research*, **27**, 377–397, https://doi.org/10.1016/j.cretres.2005.07.006

Gale, A.S., Bown, P. *et al.* 2011. The uppermost Middle and Upper Albian succession at the Col de Palluel, Hautes-Alpes, France: An integrated study (ammonites, inoceramid bivalves, planktonic foraminifera, nannofossils, geochemistry, stable oxygen and carbon isotopes, cyclostratigraphy). *Cretaceous Research*, **32**, 59–130, https://doi.org/10.1016/j.cretres.2010.10.004

Garzanti, E. 2016. From static to dynamic provenance analysis – Sedimentary petrology upgraded. *Sedimentary Geology*, **336**, 3–13, https://doi.org/10.1016/j.sedgeo.2015.07.010

Gasperini, L., Bernoulli, D. *et al.* 2001. Lower Cretaceous to Eocene sedimentary transverse ridge at the Romanche Fracture Zone and the opening of the equatorial Atlantic. *Marine Geology*, **176**, 101–119, https://doi.org/10.1016/S0025-3227(01)00146-3

Geognostics 2020. *Geognostics Earth Model (GEM)*. Geognostics, https://www.geognostics.com

Gouiza, M., Bertotti, G., Charton, R., Haimoudane, K., Dunkl, I. and Anczkiewicz, A.A. 2019. New evidence of 'anomalous' vertical movements along the hinterland of the Atlantic NW African margin. *Journal of Geophysical Research: Solid Earth*, **124**, 13 333–13 353, https://doi.org/10.1029/2019JB017914

Gouyet, S. 1988. *Evolution Tectono-Sédimentaire des Marges Guyanaise et Nord-Brésilienne au Cours de l'ouverture de l'Atlantique Sud*. Doctoral thesis, Université de Pau, Pau, France.

Gouyet, S., Unternehr, P. and Mascle, A. 1994. The French Guyana margin and the Demerara Plateau: geological history and petroleum plays. *In*: *Hydrocarbon and Petroleum Geology of France*. Springer, Berlin, 411–422.

Greenroyd, C.J., Peirce, C., Rodger, M., Watts, A.B. and Hobbs, R.W. 2005. Crustal Structure of the Continental Margin Offshore French Guiana, Central Atlantic. *AGU Fall Meeting Abstracts*, **2005**, T43B–1403.

Greenroyd, C.J., Peirce, C., Rodger, M., Watts, A.B. and Hobbs, R.W. 2007. Crustal structure of the French Guiana margin, west equatorial Atlantic. *Geophysical Journal International*, **169**, 964–987, https://doi.org/10.1111/j.1365-246X.2007.03372.x

Greenroyd, C.J., Peirce, C., Rodger, M., Watts, A.B. and Hobbs, R.W. 2008. Demerara Plateau – The structure and evolution of a transform passive margin. *Geophysical Journal International*, **172**, 549–564, https://doi.org/10.1111/j.1365-246X.2007.03662.x

Griffith, C.P. 2017. Evidence for a Jurassic source rock in the Guiana–Suriname Basin. *AAPG Datapages/Search and Discovery*, 90291.

Habib, D. and Drugg, W.S. 1983. Dinoflagellate age of Middle Jurassic–Early Cretaceous sediments in the Blake–Bahama Basin. *In*: *Initial Reports of the Deep Sea Drilling Project, Volume 76*. US Government Printing Office, Washington, DC, 623–638.

Haq, B.U. 2014. Cretaceous eustasy revisited. *Global and Planetary Change*, **113**, 44–58, https://doi.org/10.1016/j.gloplacha.2013.12.007

Hardas, P. and Mutterlose, J. 2006. Calcareous nannofossil biostratigraphy of the Cenomanian/Turonian boundary interval of ODP Leg 207 at the Demerara Rise. *Revue de Micropaléontologie*, **49**, 165–179, https://doi.org/10.1016/j.revmic.2006.04.005

Hayes, D.E., Pimm, A.C. *et al.* 1972. *Initial Reports of the Deep Sea Drilling Project, Volume 14*. US Government Printing Office, Washington, DC.

Heine, C., Zoethout, J. and Müller, R. D. 2013. Kinematics of the South Atlantic rift. *Solid Earth Discussions*, **5**, 41–116, https://doi.org/10.5194/se-4-215-2013

Hill, M.E., 1976. Lower Cretaceous calcareous nannofossils from Texas and Oklahoma. *Palaeontographica Abteilung B*, **156**, 4–6, 103–179.

Jacobi, R.D. and Hayes, D.E. 1982. Bathymetry, microphysiography and reflectivity characteristics of the West African margin between Sierra Leone and Mauritania. *In*: *Geology of the Northwest African Continental Margin*. Springer, Berlin, 182–212.

James, R., Scotchman, J. and Head, R. 2020. Why is there heavy oil in Cenozoic reservoirs offshore Guyana. *Halliburton Exploration Insights*, .

Jeremiah, J. 1996. A proposed Albian to lower Cenomanian nannofossil biozonation for England and the North Sea Basin. *Journal of Micropalaeontology*, **15** , 97–129, https://doi.org/10.1144/jm.15.2.97

Jeremiah, J. 2001. A Lower Cretaceous nannofossil zonation for the North Sea Basin. *Journal of Micropalaeontology*, **20**, 45–80, https://doi.org/10.1144/jm.20.1.45

Kean, A.E. 2007. Guiana's Basin, a Unique Setting with Two Break-up and Drift Unconformities and a Feature Hypothesized to be a Southern North Atlantic, Iceland Equivalent Atlantis. AGU *Fall Meeting Abstracts*, **2007**, T41A–0375.

Kneller, E.A. and Johnson, C.A. 2011. Plate kinematics of the Gulf of Mexico based on integrated observations from the Central and South Atlantic. *Gulf Coast Association of Geological Societies Transactions*, **2011**, 283–300.

Kosmos Energy 2018. *Investor Presentation – March 2018*. Kosmos Energy, Dallas, TX, https://www.kosmosenergy.com/

Krauspenhar, P.M., Carvalho, M.A., Fauth, G. and Lana, C.C. 2014. Albian palynostratigraphy of ODP Leg 207 (Holes 1257A, 1258C and 1260B), Demerara Rise, Equatorial Atlantic. *Revue de Micropaléontologie*, **57**, 1–13, https://doi.org/10.1016/j.revmic.2014.02.002

Kulhanek, D.K. and Wise, S.W.Jr 2006. Albian calcareous nannofossils from ODP Site 1258, Demerara Rise. *Revue de Micropaléontologie*, **49**, 181–195, https://doi.org/10.1016/j.revmic.2006.06.002

Kusznir, N.J., Roberts, A.M. and Alvey, A.D. 2018. Crustal structure of the conjugate Equatorial Atlantic Margins, derived by gravity anomaly inversion. *Geological Society, London, Special Publications*, **476**, 83–107, https://doi.org/10.1144/SP476.5

Labails, C., Olivet, J.L., Aslanian, D. and Roest, W.R. 2010. An alternative early opening scenario for the Central Atlantic Ocean. *Earth and Planetary Science Letters*, **297**, 355–368, https://doi.org/10.1016/j.epsl.2010.06.024

Loncke, L., Roest, W.R. *et al.* 2020. Transform marginal plateaus. *Earth-Science Reviews*, **203**, 102940, https://doi.org/10.1016/j.earscirev.2019.102940

Long, A., Cameron, N. and Sayers, B. 2018. The Guinea Marginal Plateau: Correlations from seismic and potential fields. Presented at the AAPG Europe Regional Conference, Global Analogues of the Atlantic Margin, 2–3 May 2018, Lisbon, Portugal.

Loucks, R.G., Kerans, C., Zeng, H. and Sullivan, P.A. 2017. Documentation and characterization of the Lower Cretaceous (Valanginian) Calvin and Winn carbonate shelves and shelf margins, onshore northcentral Gulf of Mexico. *AAPG Bulletin*, **101**, 119–142, https://doi.org/10.1306/06281615248

McCoss, A. 2017. Opening new oil basins: A pattern of discoveries. Search and Discovery Article #70280, 7th AAPG Annual Convention and Exhibition, 2–5 April 2017, Houston, Texas, USA.

McKenzie, D. 1978. Some remarks on the development of sedimentary basins. *Earth and Planetary Science Letters*, **40**, 25–32, https://doi.org/10.1016/0012-821X(78)90071-7

Mercier de Lépinay, M., Loncke, L., Basile, C., Roest, W.R., Patriat, M., Maillard, A. and De Clarens, P. 2016. Transform continental margins – Part 2: A worldwide review. *Tectonophysics*, **693**, 96–115, https://doi.org/10.1016/j.tecto.2016.05.038

Meyers, P.A., Bernasconi, S.M. and Forster, A. 2006. Origins and accumulation of organic matter in expanded Albian to Santonian black shale sequences on the Demerara Rise, South American margin. *Organic Geochemistry*, **37**, 1816–1830, https://doi.org/10.1016/j.orggeochem.2006.08.009

Michalík, J. and Reháková, D. 2011. Possible markers of the Jurassic/Cretaceous boundary in the Mediterranean Tethys: A review and state of art. *Geoscience Frontiers*, **2**, 475–490, https://doi.org/10.1016/j.gsf.2011.09.002

Mitchum, R.M. and Vail, P.R. 1977. Seismic stratigraphy and global changes of sea level: Part 7. Seismic stratigraphic interpretation procedure: Section 2. Application of seismic reflection configuration to stratigraphic interpretation. *AAPG Memoirs*, **26**, 135–143.

Monteil, E. 1992. Kystes de dinoflagelles index (Tithonique–Valanginien) du Sud-Est de la France. Proposition d'une nouvelle zonation palynologique. *Revue de Paleobilogie*, **11**, 299–306.

Morgan, W.J. 1983. Hotspot tracks and the early rifting of the Atlantic. *Tectonophysics*, **94**, 123–139, https://doi.org/10.1016/0040-1951(83)90013-6

Mosher, D., Erbacher, J., Zuelsdorff, L. and Meyer, H. 2005. Stratigraphy of the Demerara Rise, Suriname, South America: a rifted margin, shallow stratigraphic source rock analogue. AAPG Search and Discovery Article #90039 AAPG Annual Meeting, 16–19 June 2005, Calgary, Alberta, Canada.

Moulin, M., Aslanian, D. and Unternehr, P. 2010. A new starting point for the South and Equatorial Atlantic Ocean. *Earth-Science Reviews*, **98**, 1–37, https://doi.org/10.1016/j.earscirev.2009.08.001

Mourlot, Y. 2018. *Contrôles sur la Répartition des Argiles Organiques Dans les Bassins Profonds: cas de l'Atlantique Central au Crétacé*. Doctoral thesis, Université Toulouse III – Paul Sabatier, Toulouse, France.

Mourlot, Y., Calvès, G., Clift, P.D., Baby, G., Chaboureau, A.C. and Raisson, F. 2018. Seismic stratigraphy of Cretaceous eastern Central Atlantic Ocean: Basin evolution and palaeoceanographic implications. *Earth and Planetary Science Letters*, **499**, 107–121, https://doi.org/10.1016/j.epsl.2018.07.023

Müller, R.D., Sdrolias, M., Gaina, C. and Roest, W.R. 2008. Age, spreading rates, and spreading asymmetry of the world's ocean crust. *Geochemistry, Geophysics, Geosystems*, **9**, Q04006, https://doi.org/10.1029/2007GC001743

Nemčok, M., Rybár, S., Ekkertová, P., Kotulová, J., Hermeston, S.A. and Jones, D. 2015. Transform-margin model of hydrocarbon migration: the Guyana–Suriname case study. *Geological Society, London, Special Publications*, **431**, 199–217, https://doi.org/10.1144/SP431.6

Olyphant, J.R., Johnson, R.A. and Hughes, A.N. 2017. Evolution of the Southern Guinea Plateau: Implications on Guinea–Demerara Plateau formation using insights from seismic, subsidence, and gravity data. *Tectonophysics*, **717**, 358–371, https://doi.org/10.1016/j.tecto.2017.08.036

Owen, H.G. and Mutterlose, J. 2006. Late Albian ammonites from offshore Suriname: implications for biostratigraphy and palaeobiogeography. *Cretaceous Research*, **27**, 717–727, https://doi.org/10.1016/j.cretres.2005.12.001

Pasley, M.A., Shepherd, D.B., Pocknall, D.T., Boyd, K.P., Andrade, V. and Figueiredo, J.P. 2004. Sequence stratigraphy and basin evolution of the Foz do Amazonas Basin, Brazil. Search and Discovery Article #10082, AAPG International Conference and Exhibition, 24–27 October 2004, Cancun, Mexico.

Payton, C.E. (ed.) 1977. *Seismic Stratigraphy: Applications to Hydrocarbon Exploration*. *AAPG Memoirs*, **26**.

Pereira, R. and Alves, T.M. 2011. Margin segmentation prior to continental breakup: A seismic–stratigraphic record of multiphased rifting in the North Atlantic (Southwest Iberia). *Tectonophysics*, **505**, 17–34, https://doi.org/10.1016/j.tecto.2011.03.011

Pindell, J.L. 1985. Alleghenian reconstruction and subsequent evolution of the Gulf of Mexico, Bahamas, and proto-Caribbean. *Tectonics*, **4**, 1–39, https://doi.org/10.1029/TC004i001p00001

Remane, J., 1985. Calpionellids. In: Bolli, H.M., Saunders, J.B., Perch Nielsen, K. (eds) Plankton Stratigraphy. Cambridge University Press, 555–572.

Reuber, K.R., Pindell, J. and Horn, B.W. 2016. Demerara Rise, offshore Suriname: Magma-rich segment of the Central Atlantic Ocean, and conjugate to the Bahamas hot spot. *Interpretation*, **4**, 141–155, https://doi.org/10.1190/INT-2014-0246.1

Sapin, F., Davaux, M., Dall'Asta, M., Lahmi, M., Baudot, G. and Ringenbach, J.C. 2016. Post-rift subsidence of the French Guiana hyper-oblique margin: from rift-inherited subsidence to Amazon deposition effect. *Geological Society, London, Special Publications*, **431**, 125–144, https://doi.org/10.1144/SP431.11

Schlanger, S.O., Arthur, M.A., Jenkyns, H.C. and Scholle, P.A. 1987. The Cenomanian–Turonian Oceanic Anoxic Event, I. Stratigraphy and distribution of organic carbon-rich beds and the marine δ13C excursion. *Geological Society, London, Special Publications*, **26**, 371–399, https://doi.org/10.1144/GSL.SP.1987.026.01.24

Sheriff, R.E. 1976. Inferring stratigraphy from seismic data. *AAPG Bulletin*, **60**, 528–542.

Sheriff, R.E. 1977. Limitations on resolution of seismic reflections and geologic detail derivable from them: Section 1. Fundamentals of stratigraphic interpretation of seismic data. *AAPG Memoirs*, **26**, 3–14.

Sibuet, J.C. and Mascle, J. 1978. Plate kinematic implications of Atlantic equatorial fracture zone trends. *Journal of Geophysical Research: Solid Earth*, **83**, 3401–3421, https://doi.org/10.1029/JB083iB07p03401

Snyder, R.L. and Bish, D.L. 1989. Quantitative analysis. *In*: Bish, D.L. and Post, J.E. (eds) *Modern Powder Diffraction*. *Reviews in Mineralogy*, **20**, 101–144.

Sømme, T.O., Helland-Hansen, W., Martinsen, O.J. and Thurmond, J.B. 2009. Relationships between morphological and sedimentological parameters in source-to-sink systems: a basis for predicting semi-quantitative characteristics in subsurface systems. *Basin Research*, **21**, 361–387, https://doi.org/10.1111/j.1365-2117.2009.00397.x

Soto, M., Morales, E., Veroslavsky, G., de Santa Ana, H., Ucha, N. and Rodríguez, P. 2011. The continental margin of Uruguay: Crustal architecture and segmentation. *Marine and Petroleum Geology*, **28**, 1676–1689, https://doi.org/10.1016/j.marpetgeo.2011.07.001

Staatsolie 2013. *Suriname International Competitive Bid Round*. Suriname National Oil Company, Paramaribo, http://www.staatsolie.com/pio/images/stories/PDF/suriname_international_bidding_round2013.pdf

Stonecipher, S.A. 1999. Genetic characteristics of glauconite and siderite: Implications for the origin of ambiguous isolated marine sandbodies. *SEPM Special Publications*, **64**, 191–204.

Tallobre, C., Loncke, L. *et al.* 2016. Description of a contourite depositional system on the Demerara Plateau: Results from geophysical data and sediment cores. *Marine Geology*, **378**, 56–73, https://doi.org/10.1016/j.margeo.2016.01.003

Thibault, N. and Gardin, S. 2006. Maastrichtian calcareous nannofossil biostratigraphy and paleoecology in the Equatorial Atlantic (Demerara Rise, ODP Leg 207 Hole 1258A). *Revue de Micropaléontologie*, **49**, 199–214, https://doi.org/10.1016/j.revmic.2006.08.002

Tsikalas, F., Faleide, J.I. and Eldholm, O. 2001. Lateral variations in tectono-magmatic style along the Lofoten–Vesterålen volcanic margin off Norway. *Marine and Petroleum Geology*, **18**, 807–832, https://doi.org/10.1016/S0264-8172(01)00030-7

Ugwu-Oju, O. 2018. *Clinothems of the Cretaceous Berbice Canyon, Offshore Guyana*. Doctoral thesis, Colorado School of Mines, Golden, Colorado, USA.

Vail, P.R., Mitchum, R.M., Shipley, T.H. and Buffler, R.T. 1980. Unconformities of the North Atlantic. *Philosophical Transactions of the Royal Society Series A: Mathematical and Physical Sciences*, **294**, 137–155.

van Helden, B.G.T. 1986. Dinoflagellate cysts at the Jurassic–Cretaceous boundary, offshore Canada. *Palynology*, **10**, 181–199, https://doi.org/10.1080/01916122.1986.9989308

Watkins, D. K. and Bowdler, J.L. 1984. Cretaceous calcareous nannofossils from Deep Sea Drilling Project Leg 77, Southeast Gulf of Mexico. *In*: Buffler, R.T., Schlager, W. *et al.*. (eds) *Initial Reports of the Deep-Sea Drilling Project, Volume 77*. United States Government Printing Office, Washington, DC, 659–674.

Watkins, D.K., Cooper, M.J. and Wilson, P.A. 2005. Calcareous nannoplankton response to late Albian oceanic anoxic event 1d in the western North Atlantic. *Paleoceanography and Paleoclimatology*, **20**, PA2010, https://doi.org/10.1029/2004PA001097

Watts, A.B. and Stewart, J. 1998. Gravity anomalies and segmentation of the continental margin offshore West Africa. *Earth and Planetary Science Letters*, **156**, 239–252, https://doi.org/10.1016/S0012-821X(98)00018-1

Webster, R.E. 2004. Tropical v. temperate zone lacustrine source rocks: examples from Takutu Basin,Guyana, and General Levalle Basin, Argentina. *AAPG Datapages/Search and Discovery*, 10070.

Wheeler, H. E. 1958. Time-stratigraphy. *AAPG Bulletin*, **42**, 1047–1063.

Wilson, J.T. 1966. Did the Atlantic close and then re-open? *Nature*, **211**, 676–681, https://doi.org/10.1038/211676a0

Wimbledon, W.A., Casellato, C.E., Rehakova, D., Bulot, L.G., Erba, E., Gardin, S., Verreussel, R.M.C.H., Munsterman, D.K. and Hunt, C.O. 2011. Fixing a basal Berriasian and Jurassic/Cretaceous (J/K) boundary–is there perhaps some light at the end of the tunnel. *Rivista Italiana di paleontologia e Stratigrafia*, **117**, 295–307, https://doi.org/10.13130/2039-4942/5976

Yang, W. and Escalona, A. 2011. Tectonostratigraphic evolution of the Guyana Basin. *AAPG Bulletin*, **95**, 1339–1368, https://doi.org/10.1306/01031110106

Zinecker, M.P. and Mann, P. 2020. Mesozoic to recent tectonostratigraphy, paleogeography, and hydrocarbon prospectivity of the Guinea Plateau, northwestern Africa. *Marine and Petroleum Geology*, in press.